A-8 AQUIFER MODEL CALIBRATION

The flow and transport models for the aquifer were calibrated independently. The aquifer model boundary conditions and permeability were first adjusted to match the target potentiometric field. Subsequently, the model porosity and dispersivity were adjusted to match the solute arrival histories. Only a subset of the data presented in Section A-4 was used in the model calibration because the complete data set was too voluminous or would not provide useful information for model calibration. The specific observational data used in this calibration process are presented in Section A-8.1 along with a description of any data manipulation needed prior to model calibration. The specific data used in calibrating the aquifer model were taken from the OU 3-13 RI/BRA (DOE-ID 1997) modeling; the *Monitoring Report/Decision Summary for Operable Unit 3-13, Group 5, Snake River Plain Aquifer* report (DOE-ID 2004c); and ongoing remedial investigations at INTEC. These data included aquifer water level measurements taken during spring/summer 2004 and tritium, Tc-99, Sr-90, I-129, and nitrate concentrations observed in aquifer wells. Results of the calibration for flow and transport are presented in Sections A-8.2 and A-8.3, respectively.

A-8.1 Specific Calibration Data For the Aquifer Model

A-8.1.1 Calibration Data for the Flow Model

The aquifer flow model was calibrated to observed water level elevations obtained during summer 2004. Data were obtained in summer 2004 from all available monitoring wells on the INL Site, including INL Site and USGS wells. Water level measurements taken in the USGS wells can be found in the USGS National Water Information Storage database, and the measurements made in the INL Site wells were obtained from the WAG 10 RI/FS annual report (DOE-ID 2005b). Seventy-eight data points were used in the calibration of this aquifer flow model. The overall large-scale gradient near the INTEC facility is predominantly south/southwest. The relatively flat gradient south and west of INTEC suggests that the aquifer permeability is high in these areas. Figure A-8-1 illustrates the INL Site-wide regional gradient (contour interval = 2 m) obtained from the 2004 measurements

.

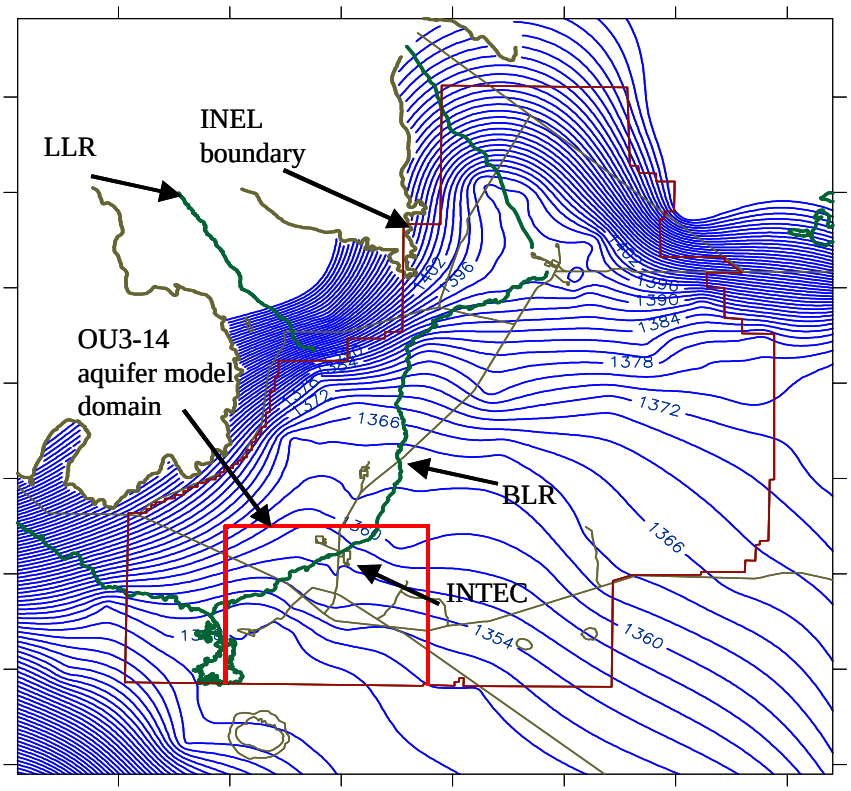

Figure A-8-1. WAG-10 regional water levels based on summer 2004 field measurements.

A-8.1.2 Calibration Data for the Transport Model

Calibration of the aquifer transport model required the magnitude of contaminant sources, the release history of the contaminants, and the concentration history in downgradient wells. The transport model was calibrated to tritium, technetium-99, strontium-90, iodine-129, and nitrate. The contaminant concentration data were obtained from the EDW.[1] The EDW is a database website maintained by the INL and contains well locations, well coordinates, water level, and water quality data. The tritium data were available in 68 wells and was most frequently sampled. The data for nitrate are most sparse, with 40 observation locations. Only wells downgradient and within the INTEC contaminant plumes were used in the model calibration.

Concentration data were first screened based on the validator-assigned data qualifier flags. If the radio analytical result was not statistically positive at the 95% confidence level, which means that the radionuclide is not present and/or the result was below minimum detection concentration in that sample, the contaminant concentration was designated nondetect. Data indicated as having severe analytical and/or quality control issues (R flags) were omitted.

The release mass and history comprising the contaminant source terms were taken from the OU 3-13 RI/BRA or estimated from historical INTEC operational records (see Section A-5.3.2). Table A-8-1 summarizes the source terms incorporated in the aquifer model. The CPP-3 injection well was the source of the

1. Idaho National Laboratory, Bechtel BWXT Idaho, LLC, *Environmental Data Warehouse (EDW)*,http://icpweb2/edw2/ , Web page updated December 3, 2004, Web page visited December 3, 2004 (Intranet web page).

early releases of contaminants in the aquifer and is the source of contaminants currently appearing in the far downgradient wells near the CFA and also of the contaminants appearing very early in wells nearer INTEC. The aquifer model sources for each simulated contaminant are presented below.

Table A-8-1 Total source mass or activity used in the vadose zone and aquifer models..

Contaminant	Injection Well Source	Percolation Pond Source	Tank Farm Source
Tritium (in Ci)	20,100	999	9.71
Technetium-99 (in Ci)	11.9	1.13	3.56
Strontium-90 (in Ci)	24.3	0.3	18,100
Iodine-129 (in Ci)	0.86	0.08	0.00126
Nitrate (in kg)	2,830,000	1,310,000	21,200

- Tritium

The main source of tritium was the CPP-03 injection well (20,100 Ci) with minor amounts originating in the former percolation ponds and from the tank farm. Tritium is transported conservatively (non-adsorbing). There were good records of tritium discharges, and it was the focus of early sampling in the aquifer. Early sample collection and reasonably complete disposal history makes it the best target for model calibration. The tritium disposal records included composite sampling of the service waste effluent (Robertson et al. 1974). In these data, tritium discharges prior to 1962 were reported as annual averages. After 1962, the data were reported as a monthly average. Even in this averaged data, there is considerable variation in discharge as shown in Figure A-8-2.

To simplify model input and to increase computational efficiency, the release history of tritium was averaged over various time periods. As shown in Figure A-8-2 for the CPP-3 injection well releases, a smaller averaging period was used when the disposal rate changed rapidly in order to preserve the general character of the data. Throughout the release history, the total amount of tritium was unchanged after applying the averaging algorithm. The period between 1968 and 1972 represents the CPP-3 injection well collapse. During this time, the discharged tritium was accounted for as releases in the vadose zone model.

- Technetium-99

The largest source of Tc-99 may have been from the CPP-03 injection well operation, with smaller amounts originating in the former percolation ponds and the tank farm. A service waste inventory for Tc-99 was not kept and as discussed in Section A-5.3.2, the amount injected at CPP-03 was estimated to be 11.9 Ci. The Tc-99 resulting from the tank farm sources was 3.56 Ci and this Tc-99 is currently entering the aquifer. The flux of vadose zone Tc-99 arriving in the aquifer is illustrated in Figure A-7-15 of Section A-7.3.1. The reported and simulated Tc-99 injection well data are given in Figure A-8-3. As shown by the averaged data incorporated into the numerical model, the discharges of Tc-99 were fairly regular throughout the operation of CPP-03 except for the time period CPP-03 was not receiving waste and during the mid-1980s.

- Strontium-90

Unlike tritium and Tc-99, the primary source of Sr-90 was associated with the tank farm releases. The amount of Sr-90 that was discharged in the CPP-03 injection well was 24.3 Ci, compared to 18,100 Ci released in the tank farm. Observations of Sr-90 in the aquifer are a direct result of the CPP-03 injection. Because of the retardation of Sr-90 in the vadose zone, the Sr-90 released in the tank farm should not reach the aquifer for several more decades. The amount of Sr-90 reaching the aquifer will be greatly attenuated because of radioactive decay and sorption. The disposal history for Sr-90 in the CPP-3 injection well is fairly complete as

illustrated in Figure A-8-4. As with tritium, these releases were smoothed using an averaging process to facilitate incorporation into the numerical model. The Sr-90 aquifer model calibration results are presented in Appendix J.

- Iodine-129

The primary source of I-129 was released via direct injection in CPP-03. It travels as a conservative contaminant and has a relatively long half-life. Total discharges to the CPP-03 injection well were 0.86 Ci compared to 0.00126 Ci originating in the tank farm. This difference illustrates that the I-129 observed in the aquifer was a direct result of the CPP-03 operation. As illustrated in Figure A-8-5, the discharge rate of I-129 in CPP-03 was relatively constant and is nearly identical in form to that of Tc-99.

- Nitrate

Concentrations of nitrate contained in the service waste are relatively constant based on long-term averages. The release rate of nitrate is variable and is a function of the service waste water volumes. Direct injection of nitrate accounts for 2,830,000 kg and is almost matched by the 1,310,000 kg estimated to be discharged via the former percolation ponds. As with I-129 and tritium, nitrate travels as a conservative constituent, which, means the surface releases may also have a significant impact on aquifer concentrations. Figure A-8-6 illustrates the estimated and simulated nitrate disposal history in the CPP-03 injection well.

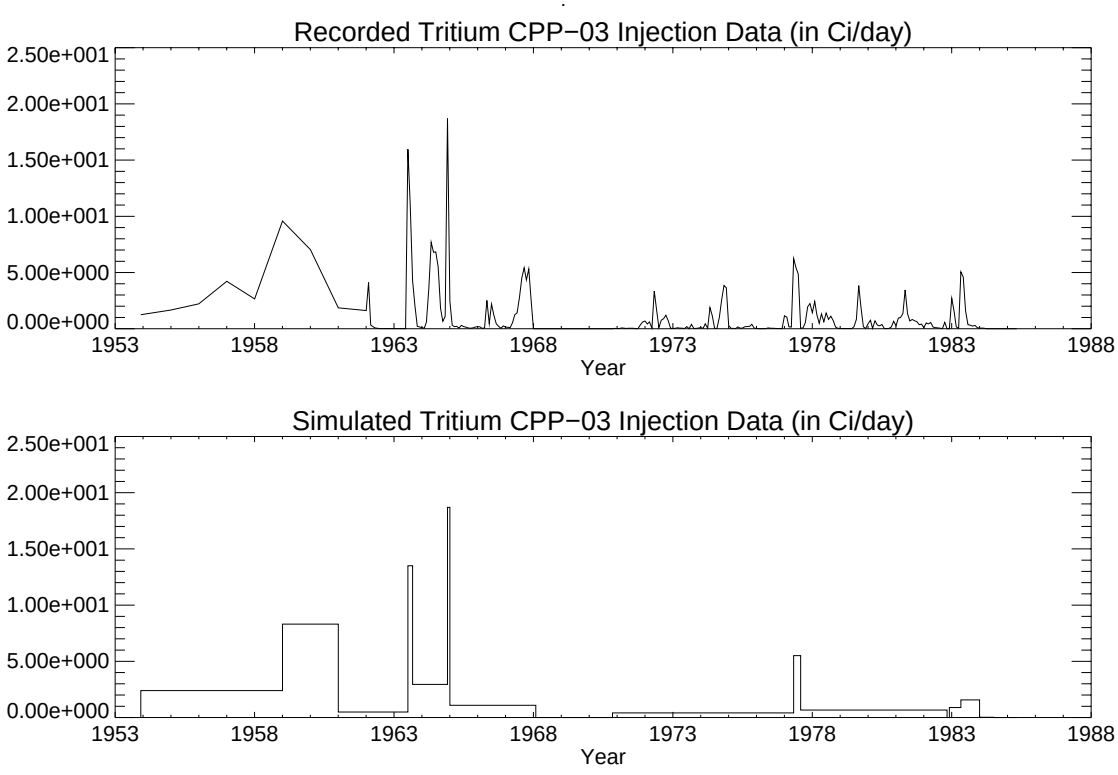

Figure A-8-2. Reported and simulated tritium disposal in CPP-03 (Ci/day).

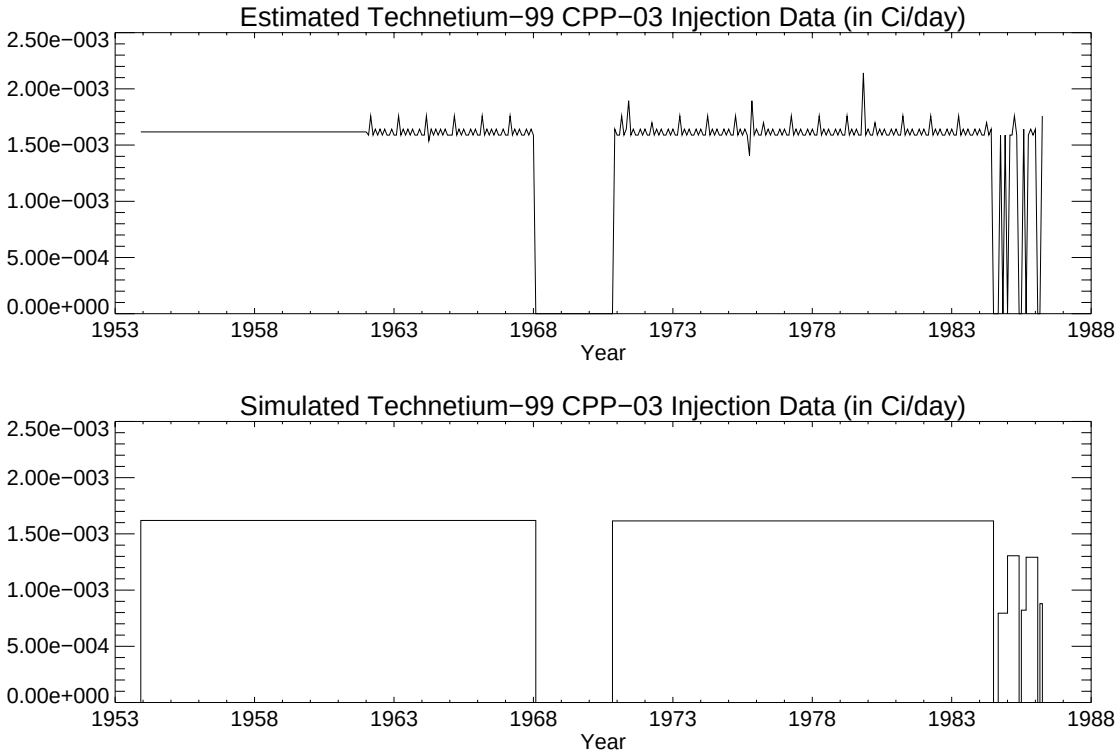

Figure A-8-3. Reported and simulated technetium-99 disposal in CPP-03 (Ci/day).

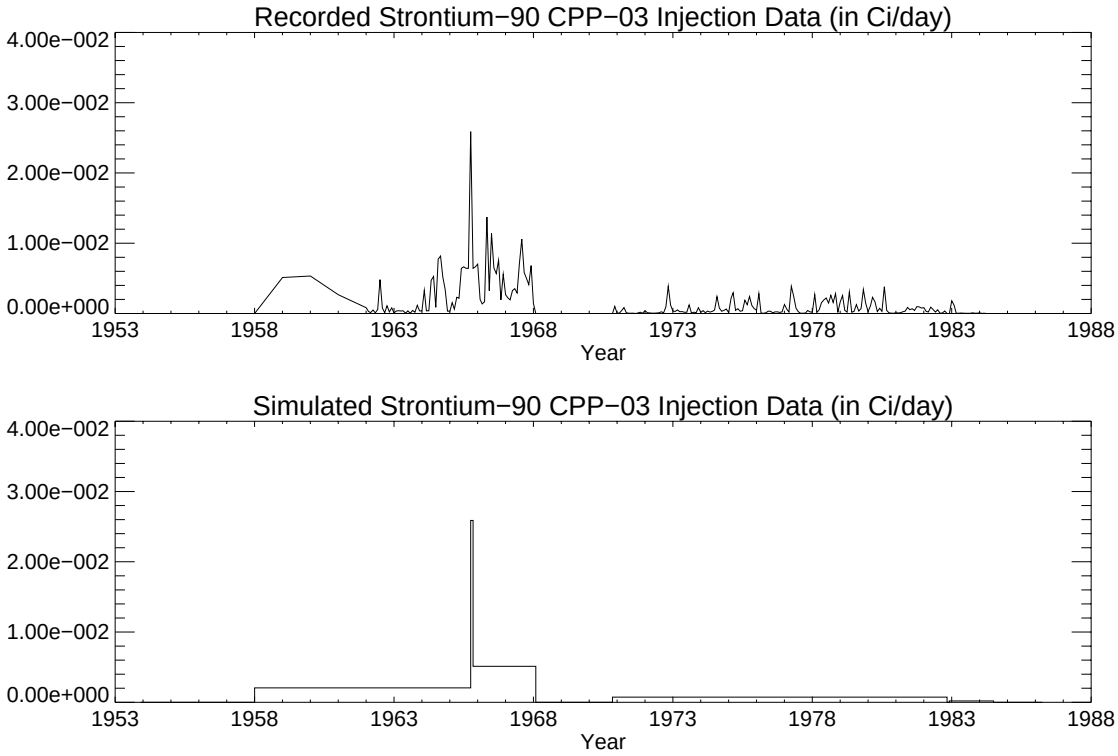

Figure A-8-4. Reported and simulated strontium-90 disposal in CPP-03 (Ci/day).

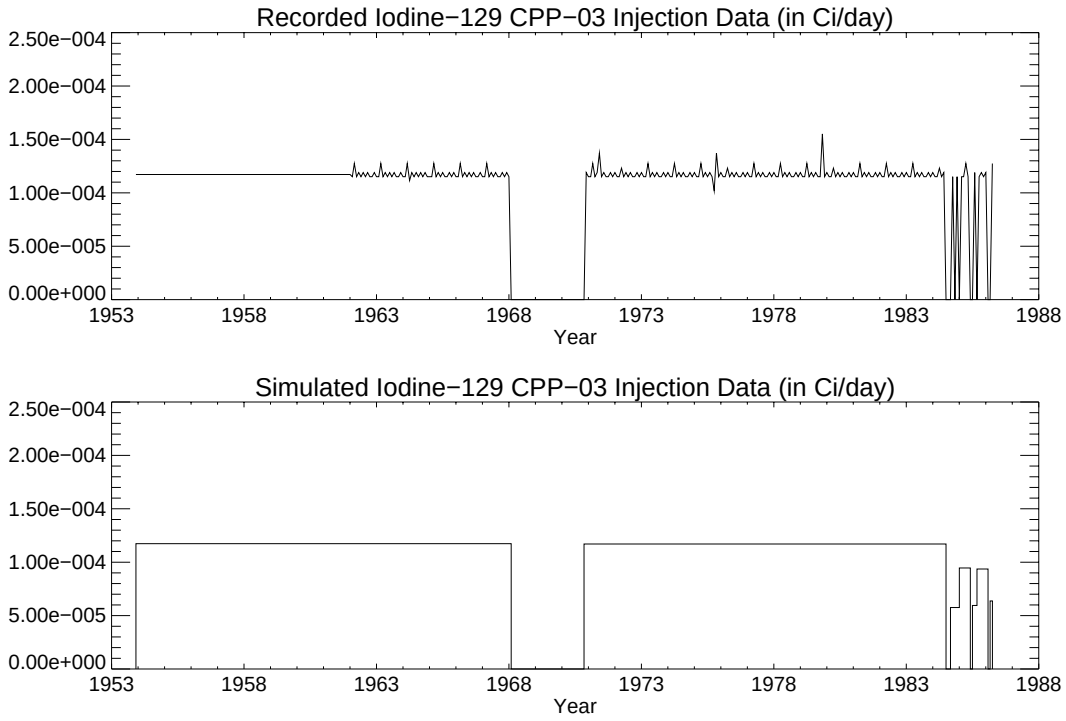

Figure A-8-5. Reported and simulated iodine-129 disposal in CPP-03 (Ci/day).

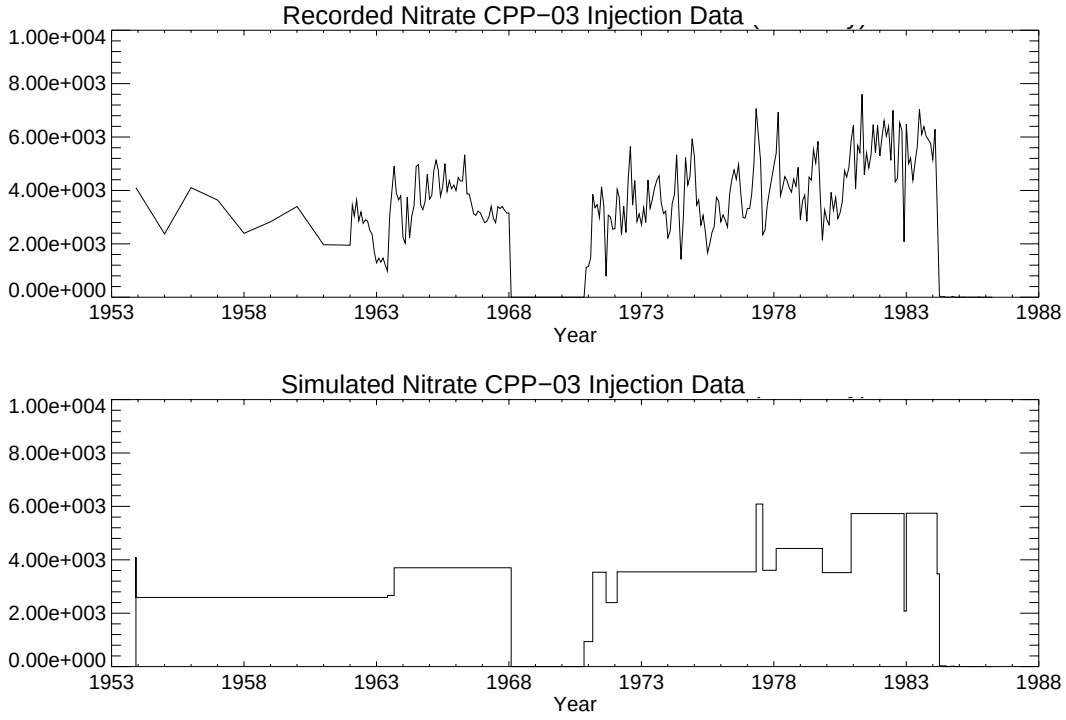

Figure A-8-6. Reported and simulated nitrate disposal in CPP-03 (kg/day as N).

A-8.2 Aquifer Flow Calibration

The aquifer flow model was calibrated to the potentiometric surface based on data from summer 2004. This was achieved by adjusting the model's steady-state Dirichlet (prescribed heads) boundary conditions and performing global adjustment of the aquifer model's permeability in each of the three lithologic layers. The boundary conditions for the aquifer model were first interpolated onto the model grid from the summer 2004 potentiometric field. To obtain a better match, the boundary heads were slightly adjusted in the northwest and along the east side. To match the heads on the interior of the flow domain, the permeability of the H basalt was then increased by a factor of two over the values presented in Section A-5.5.1, and the permeability of the I basalt was decreased by a factor of two. Hydraulic parameters for this stage in calibration are presented in Table A-8-2. The predicted and observed hydraulic heads in the layer corresponding to the top of the model are presented in Figures A-8-7 and A-8-8.

Table A-8-2 Calibrated aquifer model parameters.

Material Type	Permeability[a] (mD)	Hydraulic Conductivity (ft/day)	Porosity
H basalt	Ranging from 1.0e+3 to 1.7e+6	Ranging from 2.28E+0 to 3.87E+3	0.03
HI interbed	5.0e+2	1.14E+0	0.5
I basalt	4.e+4	1.00E+2	0.03
a. A groundwater temperature of 15 C and the Gottfried viscosity relationship to temperature was used to calculate permeability.			

The large-scale gradient is primarily south through INTEC with a slight westerly component. The flat gradient west of INTEC indicates the presence of a high-permeability zone, which is consistent with the pump test data used to parameterize the initial H basalt permeability. The regional gradient illustrates that the contamination from the INTEC should remain east of the SDA.

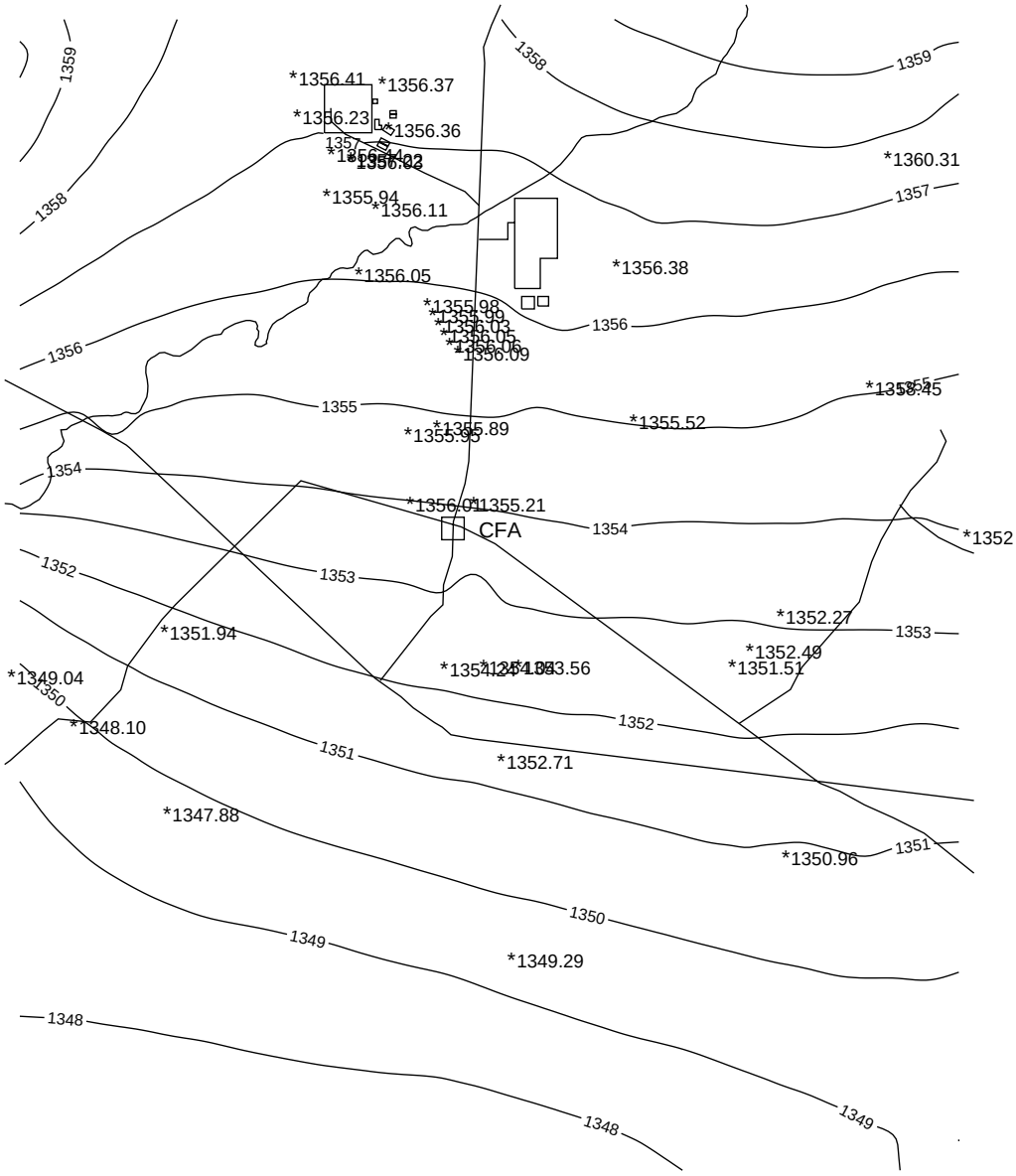

Figure A-8-7. Predicted hydraulic head (m) and summer 2004 observations (contours represent simulated values and asterisks represent observed values).

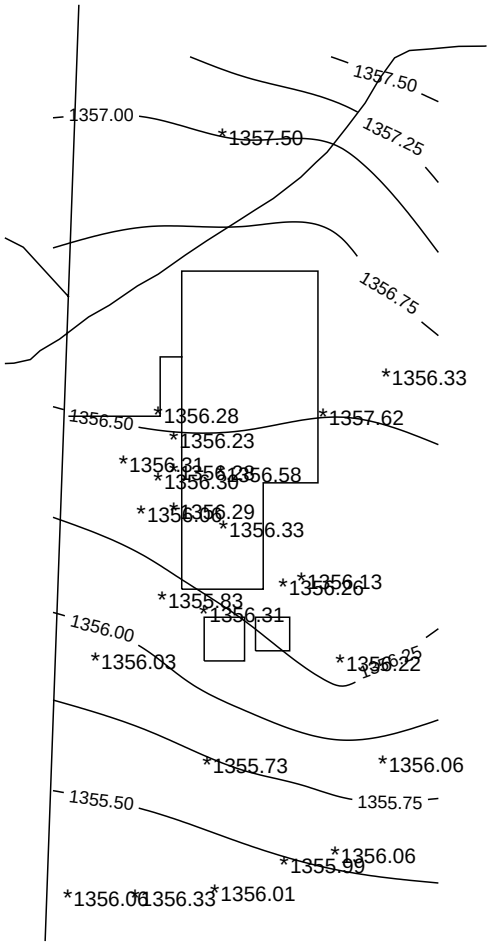

Figure A-8-8. Predicted hydraulic head (m) with summer 2004 observations near INTEC (contours represent simulated values and asterisks represent observed values).

Quantitative evaluation of the calibration was based on the RMS error which provides an estimation of the average error throughout the data set (see Section A-6). The model's overall RMS error in hydraulic head was 0.99 m (3.24 ft).

A-8.3 Aquifer Transport Model Calibration

The primary objective of the aquifer model's transport calibration was to match the timing and concentration of contaminant arrival in wells downgradient of the CPP-3 injection well, percolation ponds, and tank farm. The aquifer model was calibrated to H-3, Tc-99, and Sr-90. Because of limited sample data, model predictions were only compared to observed I-129 and nitrate. Tritium was the primary target because of the fairly certain source term, because its source is associated primarily service waste, and because the service waste stream was regularly monitored. Tritium is also the most frequently monitored contaminant in most aquifer wells. The Sr-90 calibration is presented in Appendix J along with the geochemical model development.

The dispersivity was adjusted to match the observed aquifer plume width and downgradient concentrations. In the area near INTEC, representative of short-distance and short-duration transport, the dispersivity was zero. In the area outside of the vadose zone footprint, where residence- and travel-times were longer, the resultant values were 40 m in the longitudinal direction and 20 m in the transverse. The effective dispersivity is larger than the specified values because of numerical dispersivity, and a 0-m dispersivity near INTEC resulted in sufficient solute spreading to match the observed concentrations. To match contaminant history for the calibrating targets, the permeability was increased by a factor of two over the calibrated flow model values, and a porosity of 3% was used. A summary of the calibrated aquifer model's transport parameters is presented in Table A-8-3.

Matching both the contaminant concentration and velocity required using 3% porosity for the fractured basalt within the aquifer. This is 1/2 of the value used in Appendix F of the OU 3-13 RI/BRA (DOE-ID 1997) aquifer model. The reduction was needed because OU 3-13 model used a constant 76-m thickness and the OU 3-14 model used the aquifer thickness obtained from the temperature profiles (discussed in Sections A-4.1 and A-5.2). The aquifer thickness ranged from 25 to 375 m. The much thicker aquifer required a smaller 3% porosity to match the tritium plume. The 3% porosity was consistent with the final model applied at TAN where a variable-thickness aquifer was also assumed (Martian 1999).

Locations for each of the wells used in the calibration are illustrated in Figures A-8-9 and A-8-10 for wells nearer and further away from INTEC, respectively. Resultant concentration histories for each calibration contaminant are presented in Sections A-7.3.1 through A-7.3.5. The order of presentation in each section corresponds to the distance of the wells to the CPP-3 injection well. In each figure, four data sets are presented. These include: (1) measured concentrations represented by a thin black line with a cross data symbol, (2) simulated data corresponding to the well screen center represented by a thick red line, (3) simulated concentration at the top of the aquifer represented by a thin dashed green line, and (4) simulated concentration at the aquifer bottom represented by a thin blue line. The calibration statistic was calculated for each well by comparing the values between the simulated screen center value to the observed concentration.

Table A-8-3 Calibrated aquifer model transport parameters.

Contaminant	Interbed K_d	Basalt K_d	Vadose Zone Footprint Dispersivity		Dispersivity External to Vadose Zone Footprint	
	(mL/g)	(mL/g)	Longitudinal (m)	Transverse (m)	Longitudinal (m)	Transverse (m)
Tc-99	0.	0.	0.	0.	40.	60.
Sr-90	22.	0.035	0.	0.	40.	60.
I-129	0.	0.	0.	0.	40.	60.
H-3	0.	0.	0.	0.	40.	60.
Nitrate	0.	0.	0.	0.	40.	60.

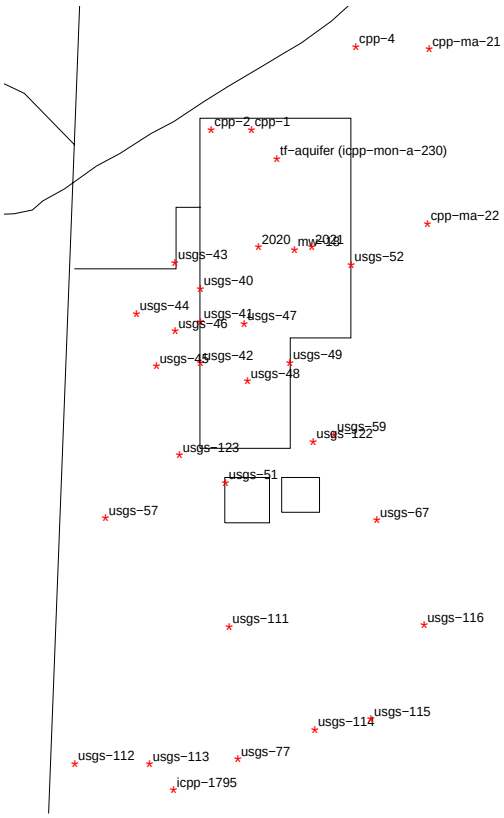

Figure A-8-9. Aquifer wells located near INTEC.

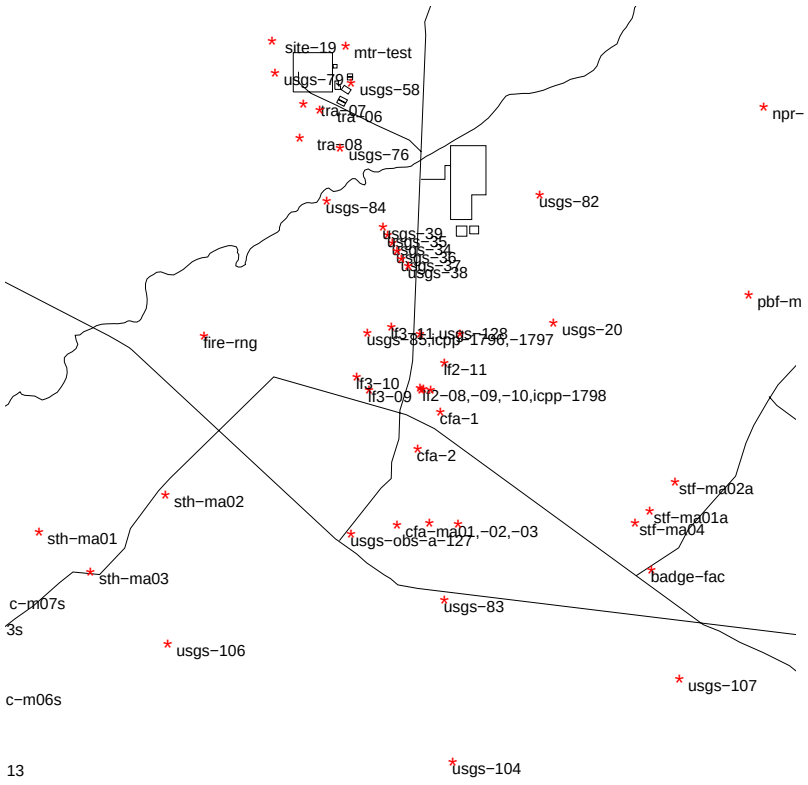

Figure A-8-10. Aquifer wells located far from INTEC.

A-8.3.1 Tritium in the Aquifer

Tritium is present in most groundwaters and the background concentration is approximately 100 pCi/L in the Snake River Plain Aquifer (Orr et al. 1991). The simulated concentrations were adjusted to account for the background concentrations by adding this amount to the predicted value.

The highest observed tritium concentration occurred in 1963 and was found in wells nearest the injection well (USGS-041 and USGS-047). These wells should respond rapidly to spikes in tritium disposal. The observed tritium concentrations in wells south and west of the INTEC tended to be higher than the simulated values, and they may have been impacted by the RTC injection well and the RTC warm waste pond. Although the RTC and INTEC plumes may merge in these areas, only the INTEC contaminant sources were considered in the model calibration. The model matches the history in most downgradient wells.

Vertical sampling for tritium was performed in 2002 in the ICPP-179x series wells (DOE-ID 2004c). These data suggest that the HI interbed may be acting as a weak confining layer between the shallow and deep aquifer. Concentrations in the vertically sampled wells were higher than predicted by the model. This suggests that the vadose zone tritium sources may have been underestimated. The tritium from the injection well had moved far south of those locations by 2002. A plan view of the maximum simulated tritium concentrations at any depth averaged over a 15-m well screen is given in Figure A-8-11. For the same year, a vertical profile through the ICPP-1795, -1796, -1797, and -1798 wells located between INTEC and CFA is given in Figure A-8-12. The average RMS error for the tritium calibration is 0.67 and the average correlation coefficient is 0.37. Wells with only one field measurement have a zero correlation reported because the correlation coefficient calculation requires at least two points. Figures A-8-13 through A-8-17 illustrate the model-predicted concentration histories with the observed data at each well location.

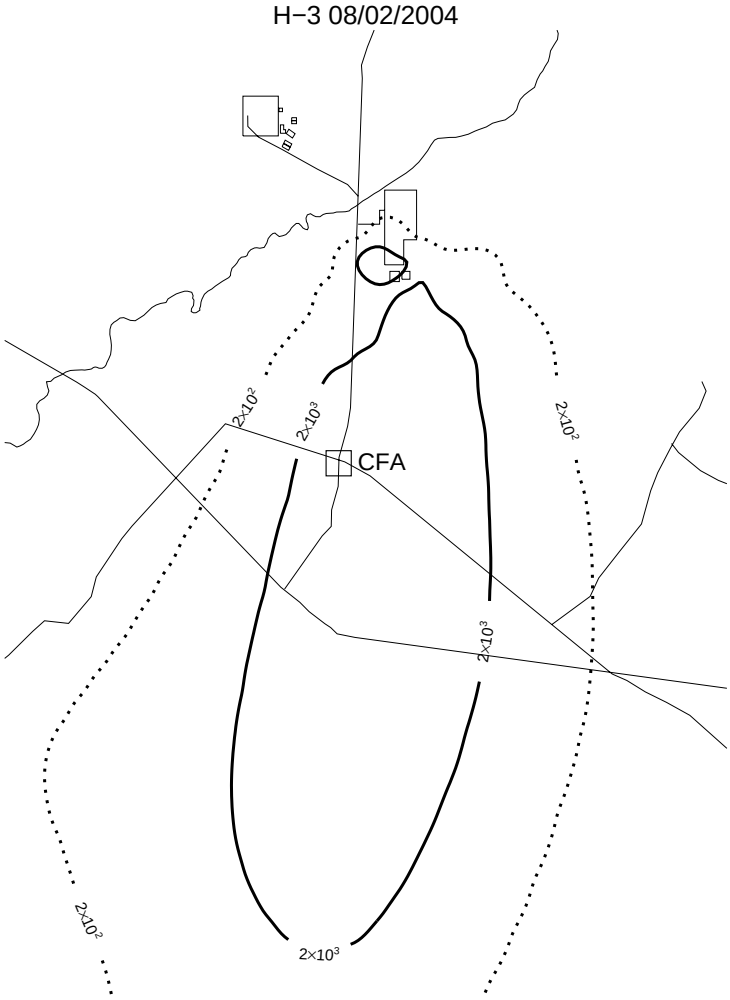

Figure A-8-11. Maximum simulated tritium (pCi/L) concentrations in base grid averaged over a 15-m well screen in 2004 (MCL=thick red line, 10*MCL=thin red line, MCL/10=thin black line, MCL/100=dashed black line).

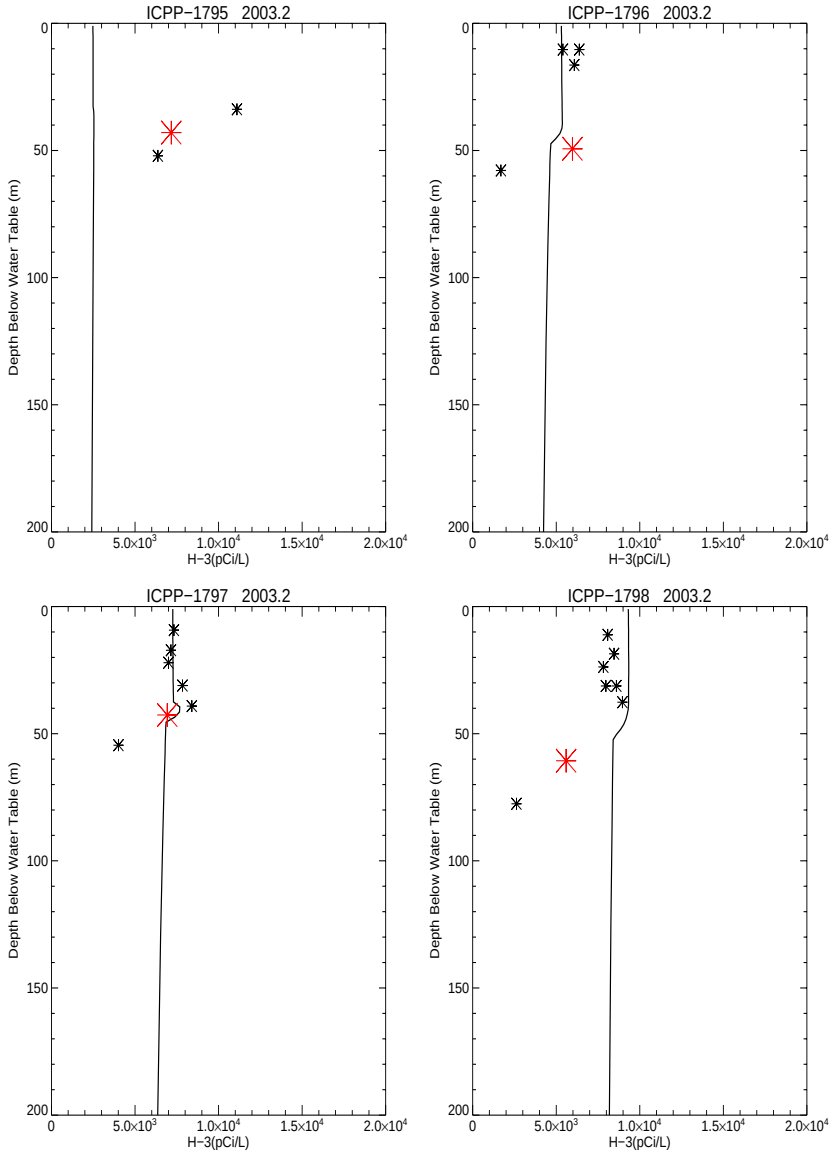

Figure A-8-12. Simulated and measured tritium vs. depth at vertical boreholes in 2003 (pCi/L) (simulated data = solid line, small asterisk = data taken in basalt, large red asterisk = data taken in the HI interbed).

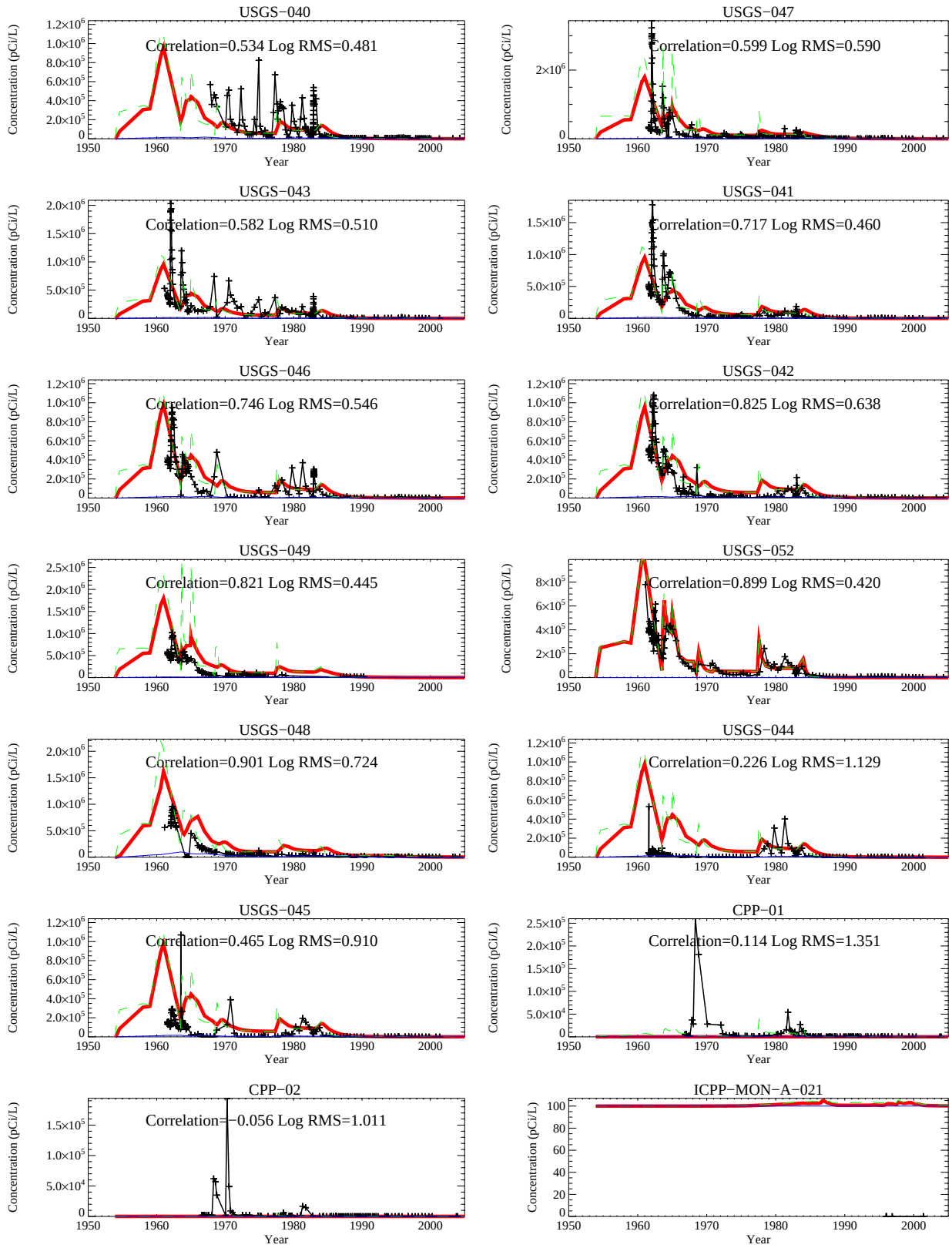

Figure A-8-13. Simulated and observed tritium concentration histories (pCi/L) (measured = black crosses, thick red = model at screen center, dashed green = model top, blue = model bottom).

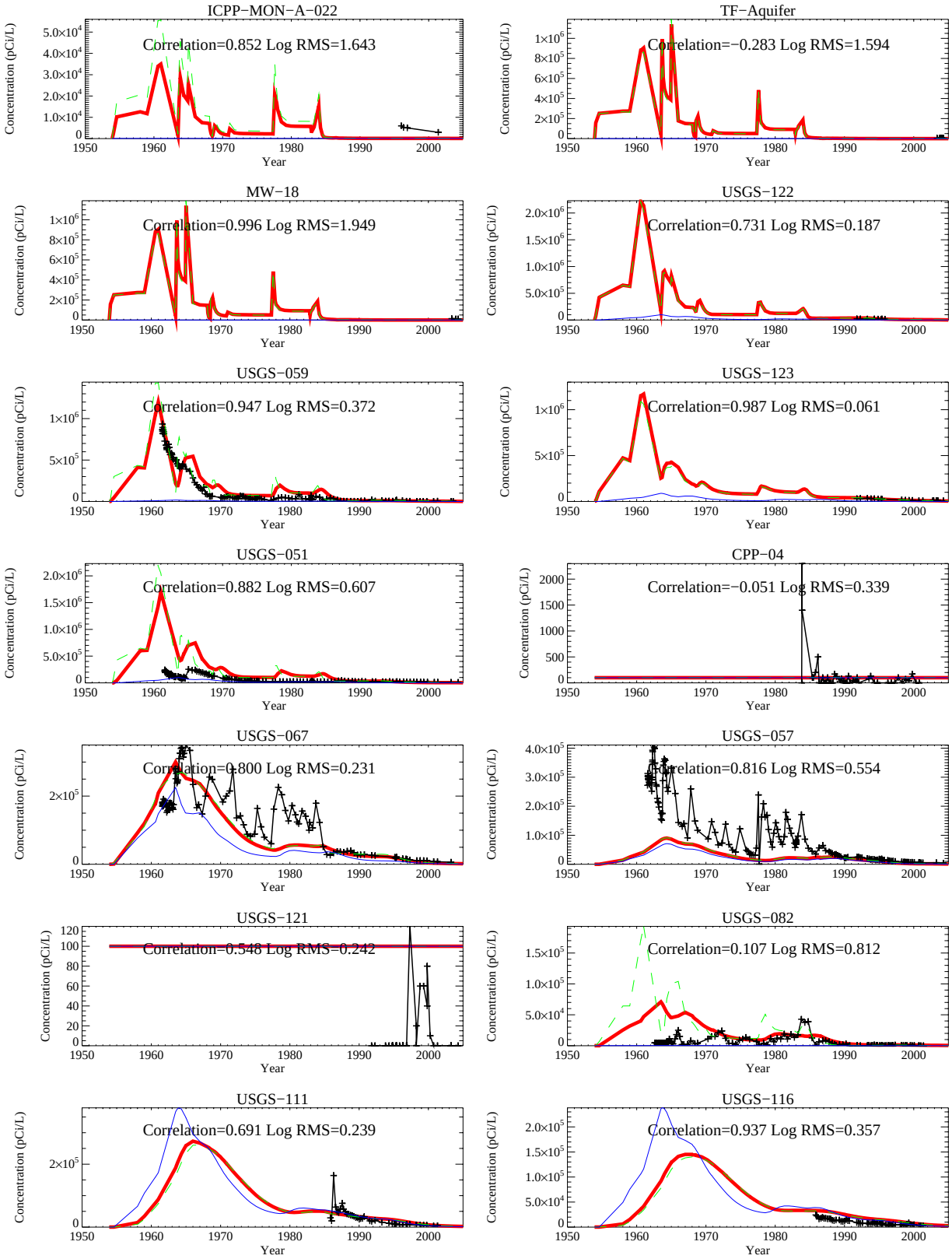

Figure A-8-14. Simulated and observed tritium concentration histories (pCi/L) (measured = black crosses, thick red = model at screen center, dashed green = model top, blue = model bottom).

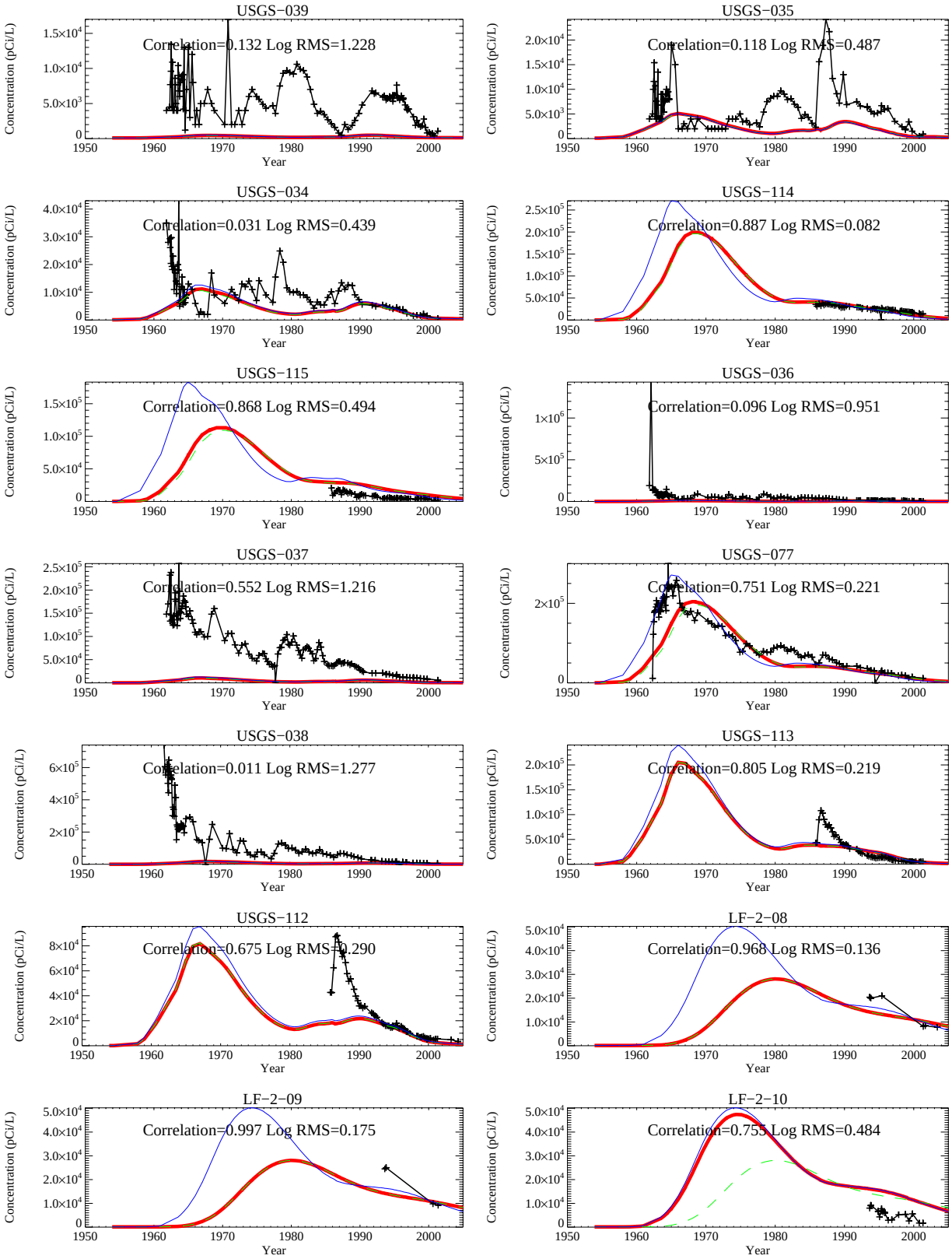

Figure A-8-15. Simulated and observed tritium concentration histories (pCi/L) (measured = black crosses, thick red = model at screen center, dashed green = model top, blue = model bottom).

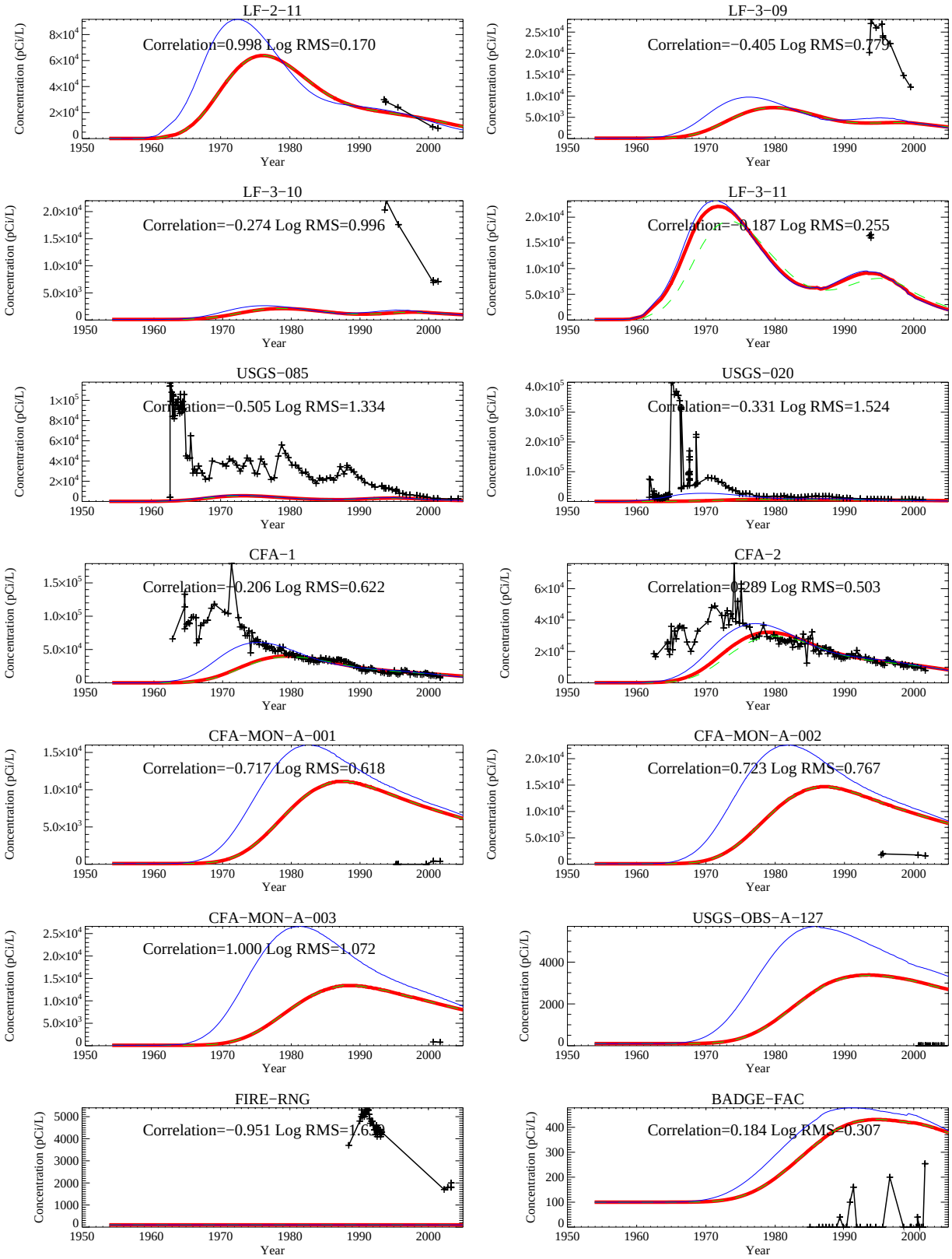

Figure A-8-16. Simulated and observed tritium concentration histories (pCi/L) (measured = black crosses, thick red = model at screen center, dashed green = model top, blue = model bottom).

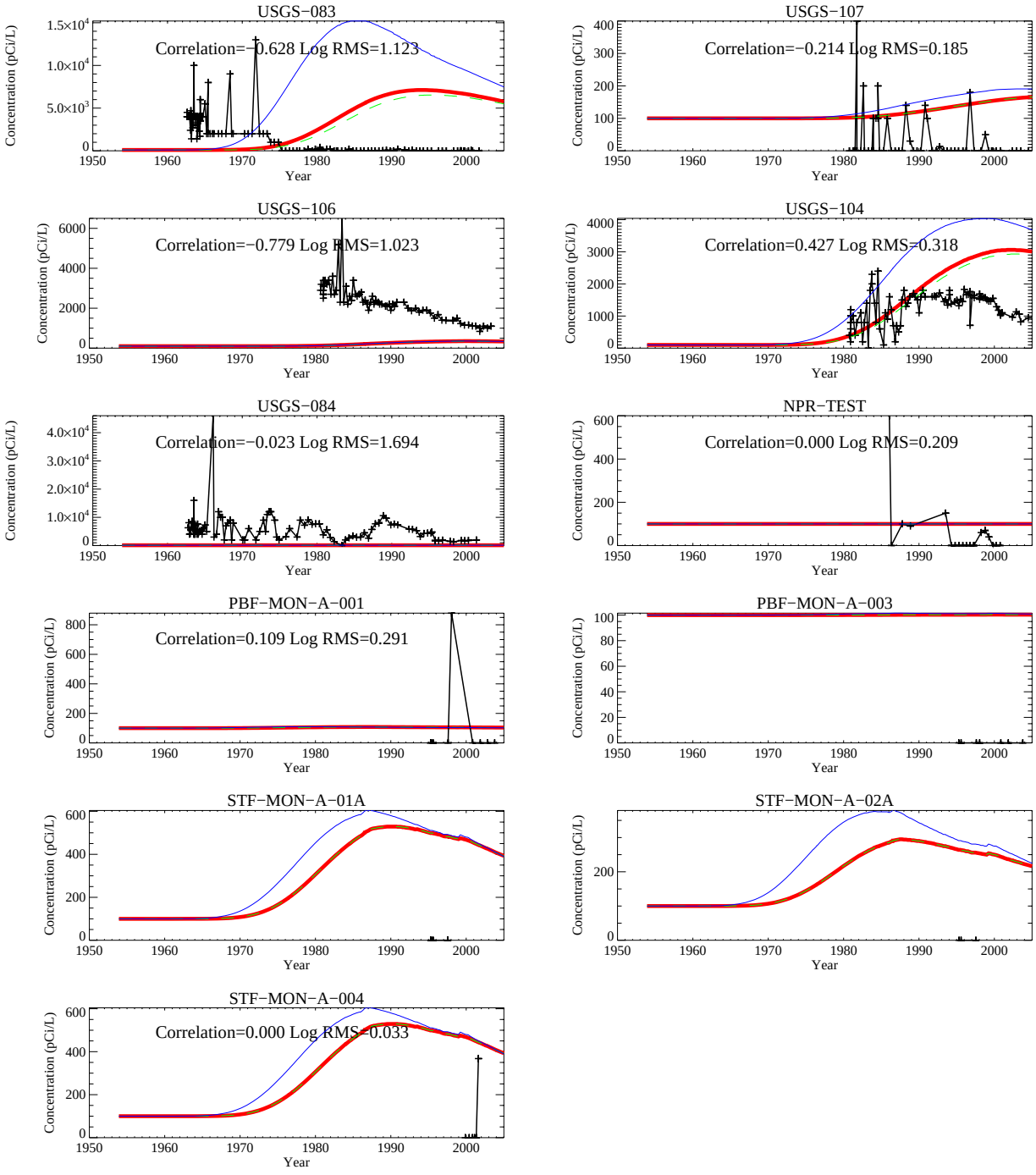

Figure A-8-17. Simulated and observed tritium concentration histories (pCi/L) (measured = black crosses, thick red = model at screen center, dashed green = model top, blue = model bottom).

A-8.3.2 Technetium-99 in the Aquifer

Calibration targets for Tc-99 included matching downgradient concentrations resulting from CPP-3 injection well discharges and matching the current high concentrations resulting from the tank farm releases. The maximum observed Tc-99 concentration was 3,160 pCi/L in 2003 and was recorded in the TF-Aquifer well. With the exception of the TF-Aquifer well, higher concentrations occur south and southeast of the tank farm. The maximum observed concentration in well USGS-52 was 339 pCi/L in 2004, and the maximum observed concentration in well MW-18 was 589 pCi/L in 2003.

Figures A-8-18 and A-8-19 show the contour plot of simulated maximum Tc-99 concentration at any depth averaged over a 15-m well screen for the refined model grid near INTEC and the base grid, respectively. The year 1999 is shown here because that is the time period when the model is predicting the highest concentrations in the aquifer. The peak aquifer concentration corresponds to the arrival of the highest predicted fluxes from the vadose zone. There are two high concentration areas in Figure A-8-19, one within the INTEC fence line and the other one nearer CFA. The high concentrations near INTEC are due to tank farm releases, which began arriving at the aquifer during the mid-1980s. The second high-concentration area is due to service waste discharges in the CPP-03 injection well.

The peak Tc-99 concentration occurring anywhere within the aquifer averaged over a 15-m well screen is shown in Figure A-8-20. The early high concentrations are the result of the injection well operation. The concentration peak occurring in the year 1999 is due to tank farm releases and corresponds to the high flow year of the Big Lost River. The overall variability is due to the fluctuations in the injection well discharge rates, variability in the Big Lost River flow, and, in part, due to the peak value being taken from any location within the model as opposed to representing a single location. The peak concentration only briefly exceeds the MCL in 1999. This is inconsistent with the maximum measured Tc-99 concentration seen in the TF-Aquifer well and the recently drilled ICPP-2020 and ICPP-2021 wells. The vadose zone model may be overestimating the attenuation occurring within the vadose zone or may have underestimated the Tc-99 source term. Possible causes include the following: 1) using a source smaller than the actual source, 2) overestimating dilution and dispersion in the vadose zone, and 3) underestimating or not accounting for preferential arrival from high concentration regions in the vadose zone. However, the simulated concentrations were similar to the measured concentrations in the vertical profile wells, which are located south of the INTEC (Figure A-8-21). This indicates dilution dispersion in the aquifer model was adequately parameterized, because the source of the Tc-99 currently seen in these wells is from the CPP-3 injection well.

The vertical profile of observed and simulated data is given in Figure A-8-21 for 2003 in the ICPP-179x series wells located between the INTEC and the CFA. The simulated and observed Tc-99 concentration history plots presented in Figures A-8-22 through A-8-28 indicate that the wells were sampled too infrequently to allow identification of the first arrival or peak concentration in most wells. Sampling in these wells began in the mid-1990s at most locations and other sampling began in 2000. The presented concentrations correspond to the values obtained from the base grid, which is 400 by 400 m. The TETRAD software reports model results for a base grid and for each refined area in separate data files. The concentration histories were created by reading the base grid data files, which correspond to the average over the refined grid blocks within each base grid block. This results in a lower reported base grid concentration because of the large averaging volume.

Figure A-8-18. Simulated maximum Tc-99 concentrations (pCi/L) near INTEC averaged over a 15-m well screen in 1999 (MCL=thick red line, 10*MCL=thin red line, MCL/10=thin black line, MCL/100=dashed black line).

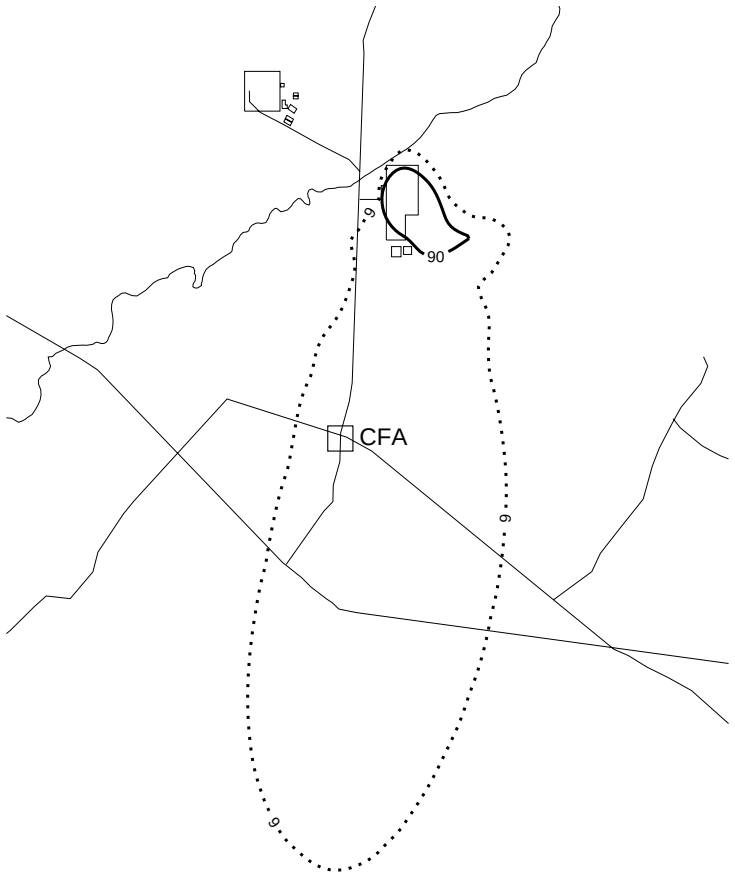

Figure A-8-19. Simulated maximum Tc-99 concentrations (pCi/L) in base grid averaged over a 15-m well screen in 1999 (MCL=thick red line, 10*MCL=thin red line, MCL/10=thin black line, MCL/100=dashed black line).

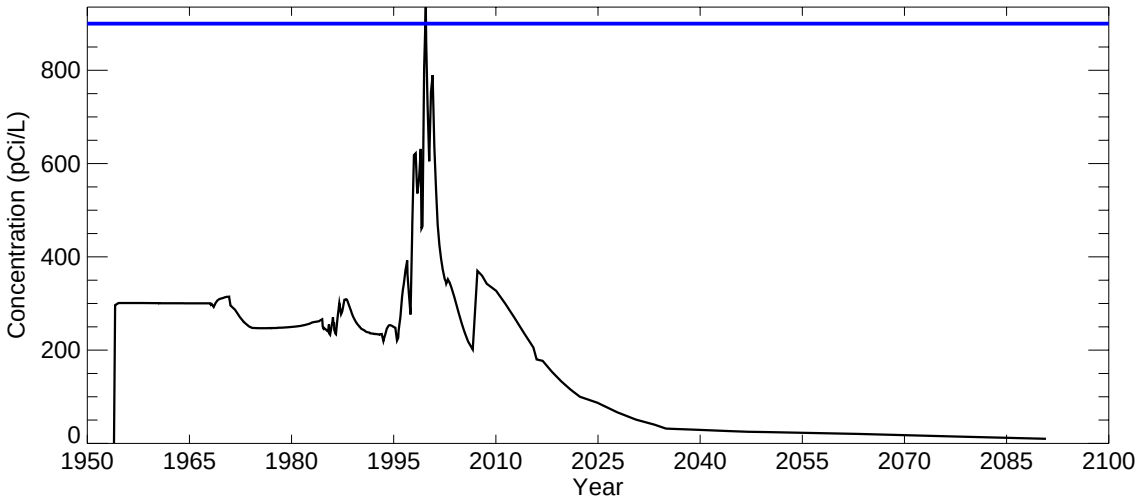

Figure A-8-20. Simulated Tc-99 peak aquifer concentrations averaged over a 15-m well screen (pCi/L).

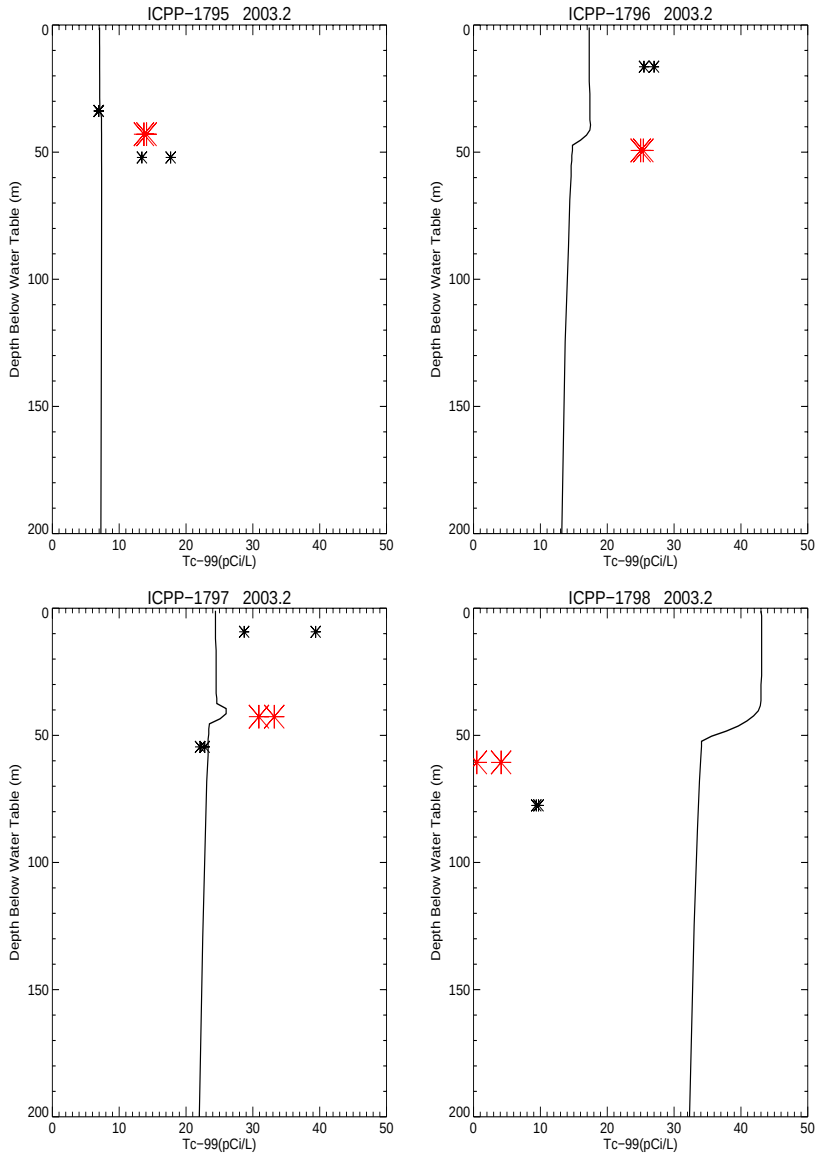

Figure A-8-21. Simulated and measured Tc-99 vs. depth at vertical boreholes in 2003 (pCi/L) (simulated data = solid line, small asterisk = data taken in basalt, large red asterisk = data taken in the HI interbed).

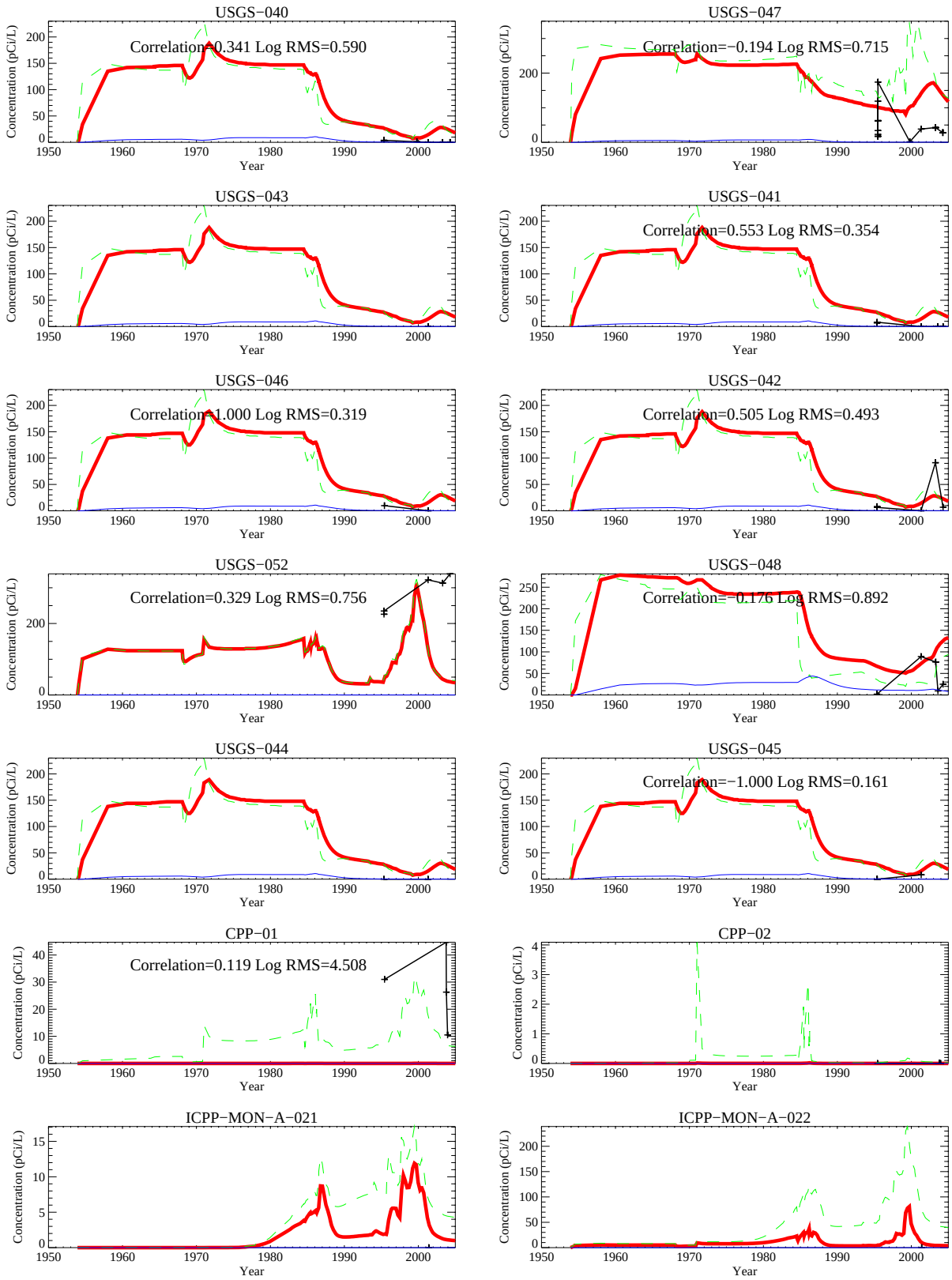

Figure A-8-22. Simulated and observed Tc-99 concentration histories (pCi/L) (measured = black crosses, thick red = model at screen center, dashed green = model top, blue = model bottom).

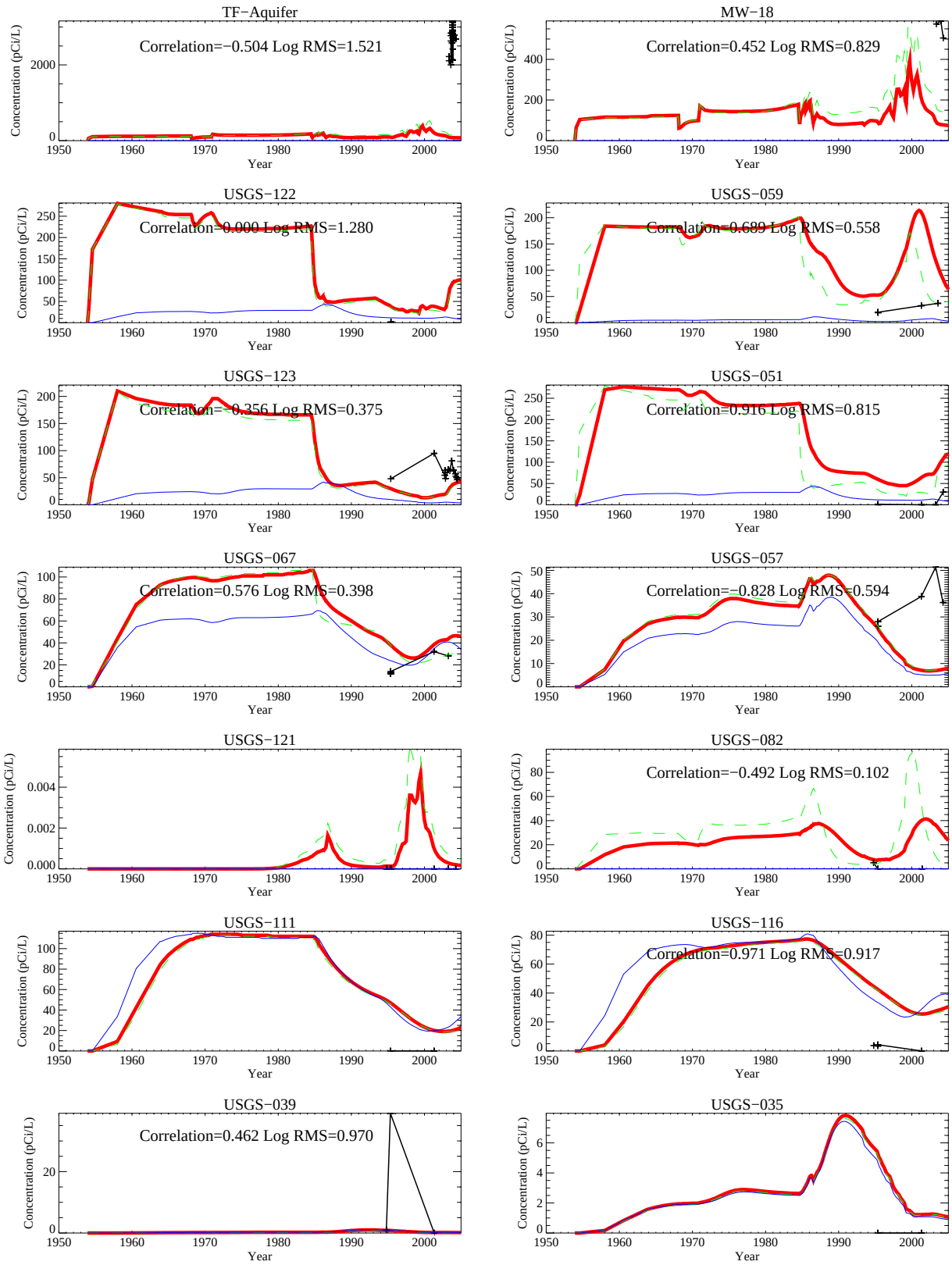

Figure A-8-23. Simulated and observed Tc-99 concentration histories (pCi/L) (measured = black crosses, thick red = model at screen center, dashed green = model top, blue = model bottom).

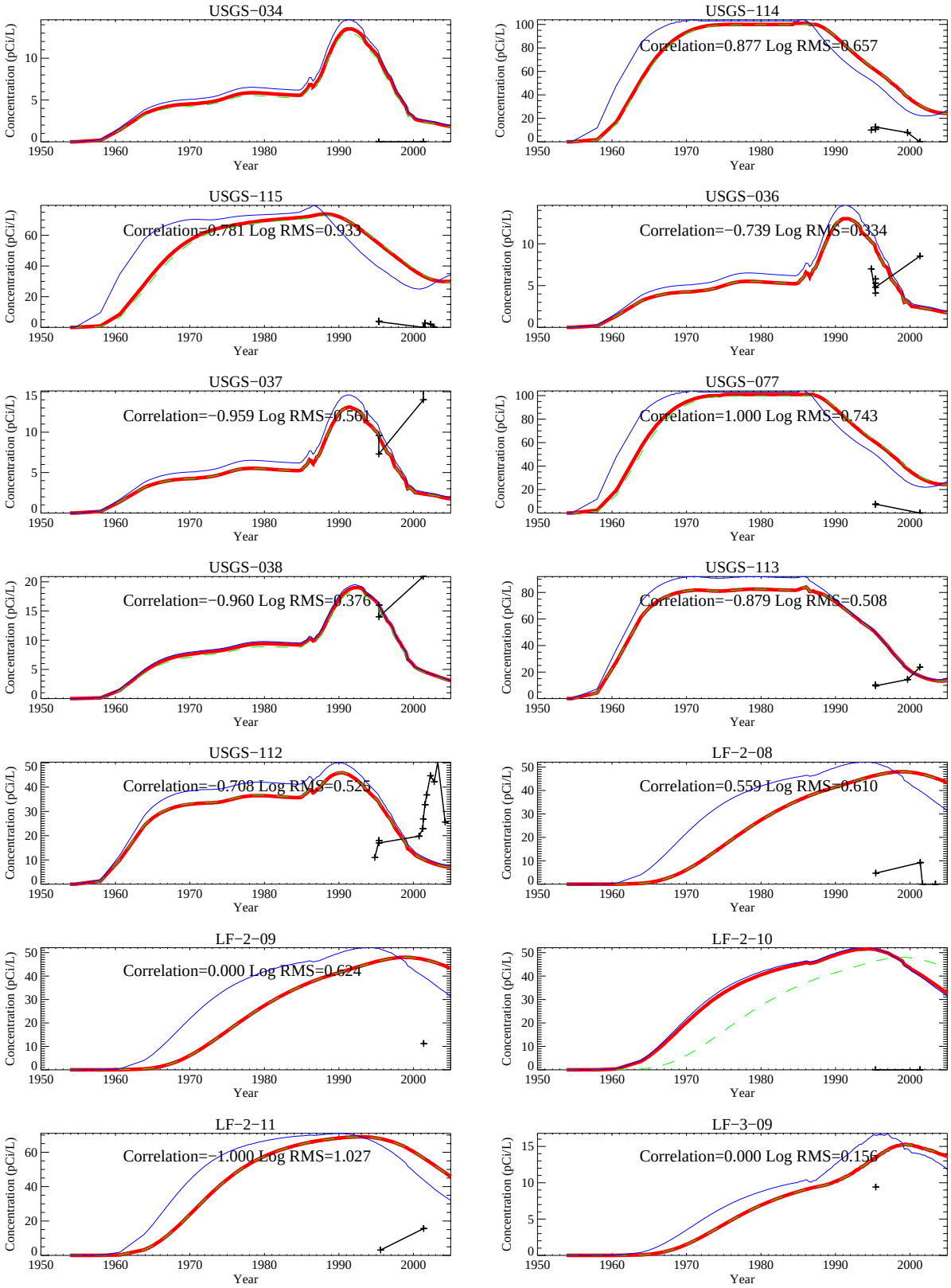

Figure A-8-24. Simulated and observed Tc-99 concentration histories (pCi/L) (measured = black crosses, thick red = model at screen center, dashed green = model top, blue = model bottom).

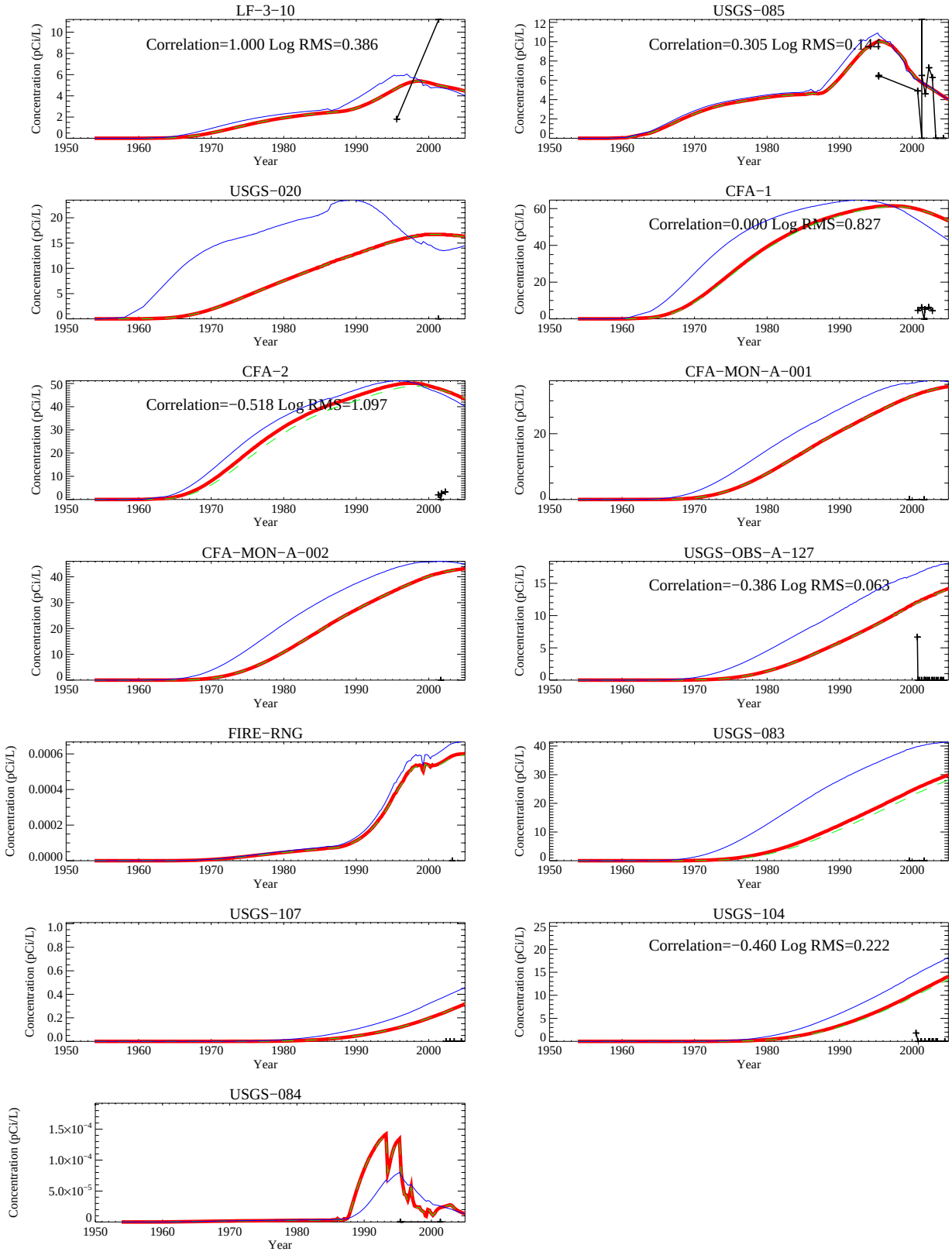

Figure A-8-25. Simulated and observed Tc-99 concentration histories (pCi/L) (measured = black crosses, thick red = model at screen center, dashed green = model top, blue = model bottom).

A-8.3.3 Iodine-129 in the Aquifer

The aquifer model was not calibrated to I-129 concentrations, but comparisons to observed data are presented. It was not used as a calibration target because the service waste disposal records were only available from 1976 through 1985. Prior to 1976, the source term used in this report was simply an estimate. The uncertainty associated with the estimated releases in the injection well were thought to be too large to use I-129 as a primary calibration target. In addition, field observations of I-129 are more sparse than data for the other calibration targets.

The aquifer model predicts that peak I-129 concentrations originating from the injection well operation reached CFA around mid-2002, as shown in Figure A-8-26. On the average, concentrations of I-129 were overpredicted in wells downgradient of CPP-3. The highest concentration observed in the most recent sampling campaign was 1.06 pCi/L and was located approximately 400 m west of CFA. Figure A-8-27 illustrates the simulated and observed vertical concentrations for 2003 in the ICPP-179x series wells located between INTEC and CFA. Figures A-8-28 through A-8-32 illustrate the simulated and observed concentrations at each well location with I-129 sampling results. There were 64 wells with observed I-129 data, but most wells have very few data points. There is more variability in the I-129 concentrations than in the injection well source term because the aquifer concentrations are also influenced by the transient injection well water disposal rate, vadose zone water flux, and arrival of the vadose zone I-129 sources. The concentration spikes seen in the measured I-129 in Wells USGS-40, 42, 44, 45, 46, and 52 may be due to an increase I-129 disposal in 1978, which coincided with low recharge from the Big Lost River. Between 1982 and 1986 the Big Lost River recharge was higher than average and waste water disposal to the injection well was stopped in 1984, thereby reducing concentrations.

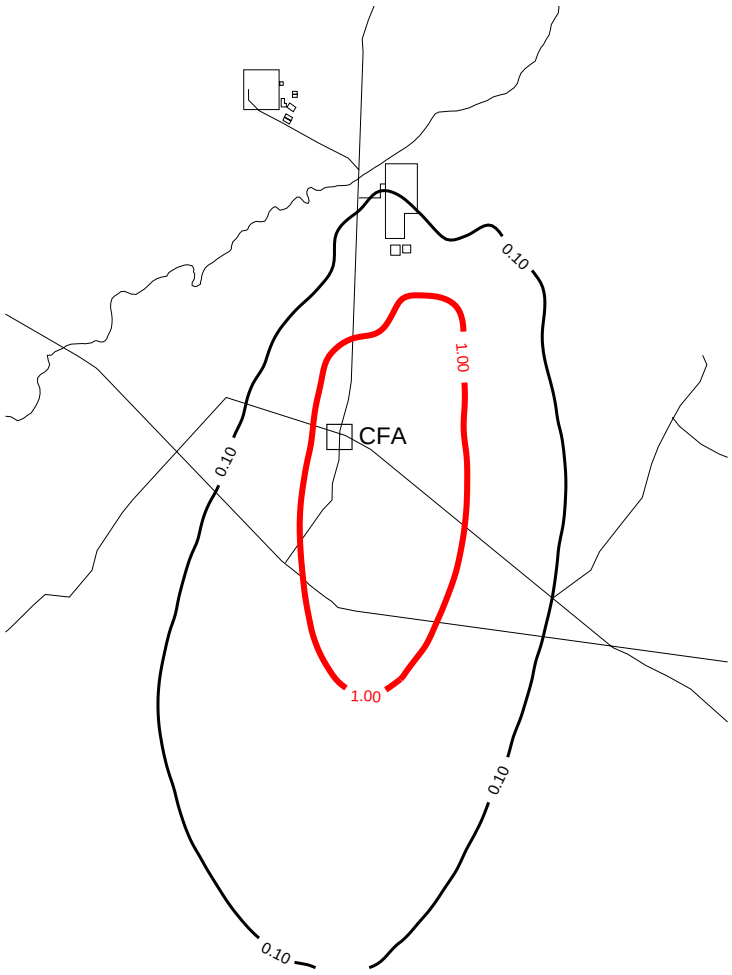

Figure A-8-26. Maximum simulated I-129 concentrations (pCi/L) in base grid averaged over a 15m well screen in 2004 (MCL=thick red line, 10*MCL=thin red line, MCL/10=thin black line, MCL/100=dashed black line).

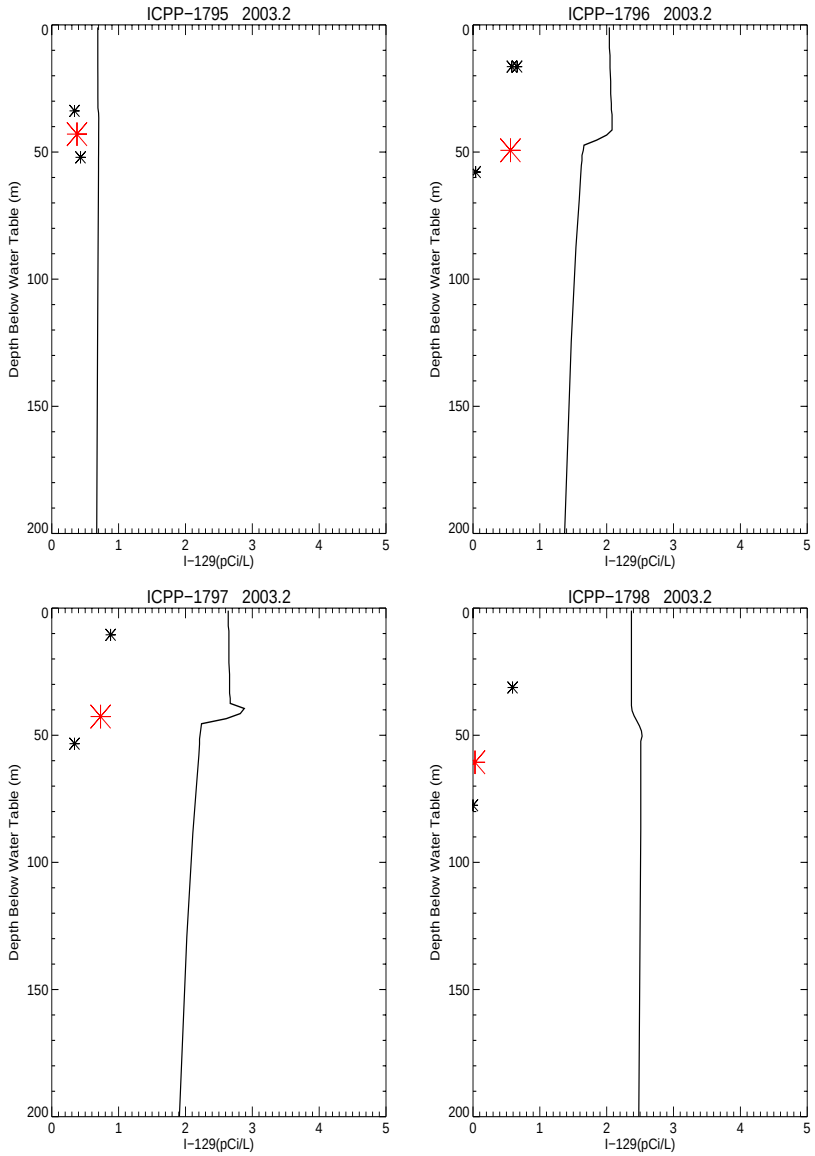

Figure A-8-27. Simulated and observed I-129 concentrations vs. depth at vertical boreholes in 2003 (simulated data = solid line, small asterisk = data taken in basalt, large red asterisk = data taken in the HI interbed, pCi/L).

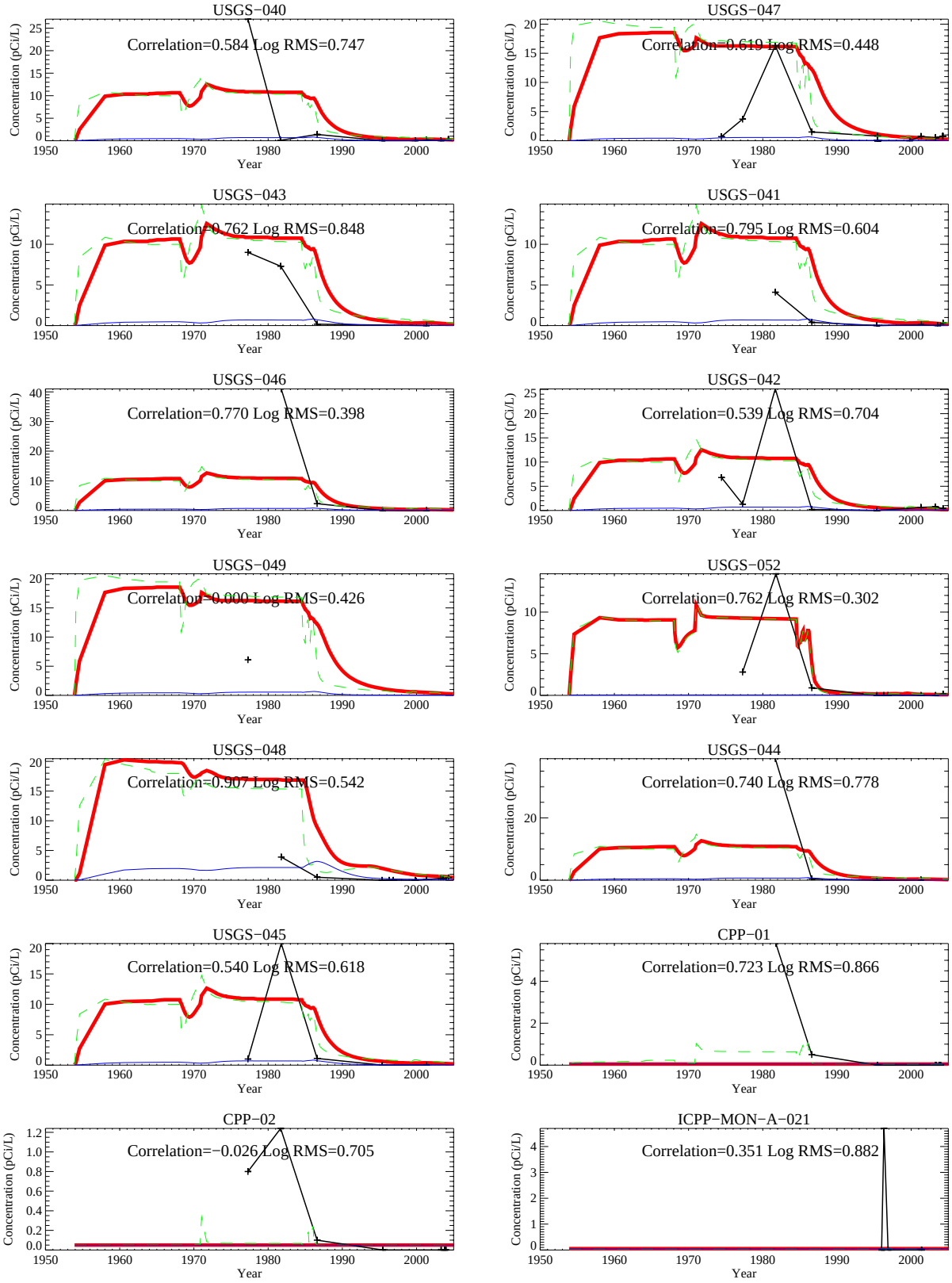

Figure A-8-28. Simulated and observed I-129 concentration histories (pCi/L) (measured = black crosses, thick red = model at screen center, dashed green = model top, blue = model bottom).

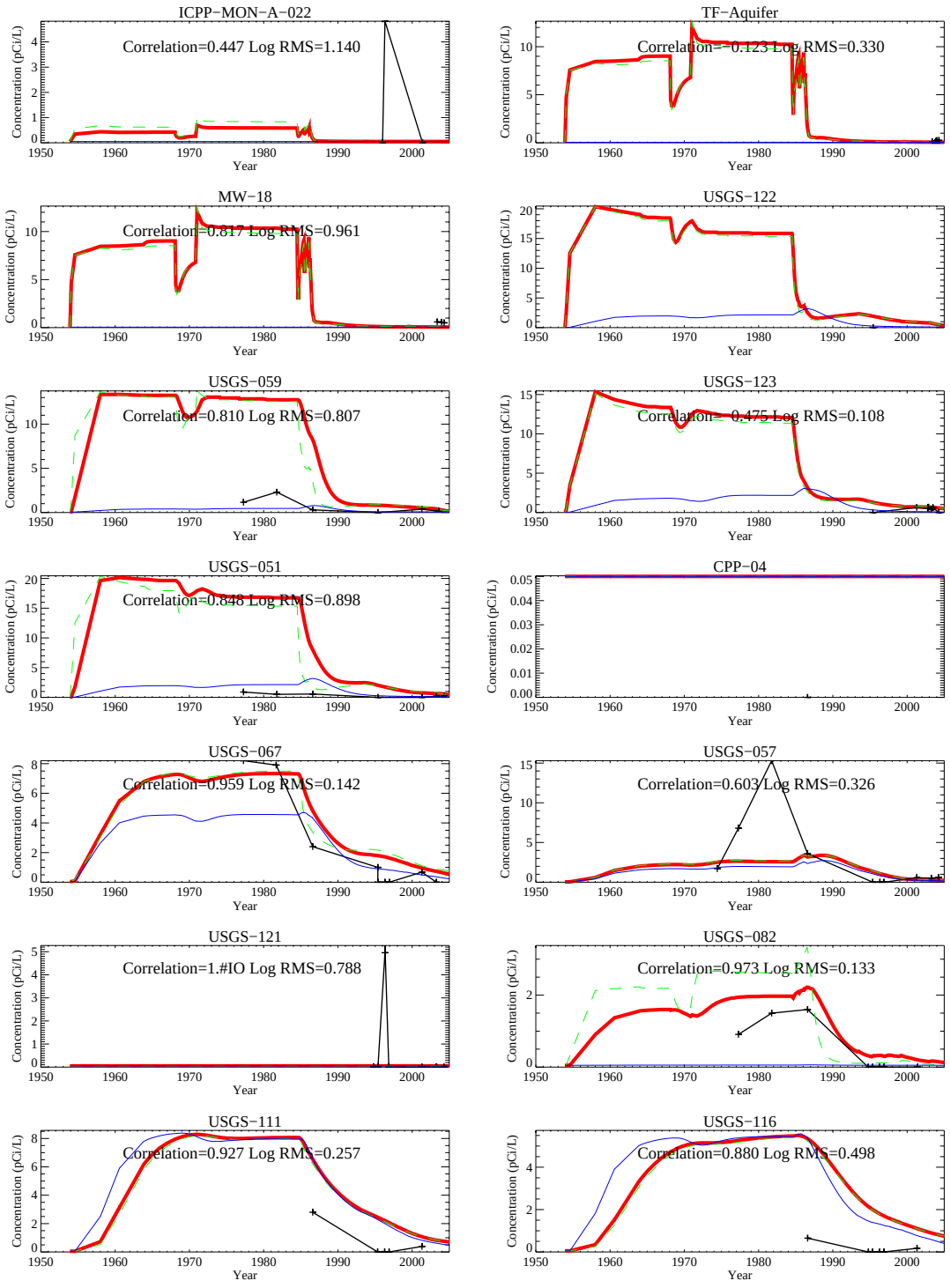

Figure A-8-29. Simulated and observed I-129 concentration histories (pCi/L) (measured = black crosses, thick red = model at screen center, dashed green = model top, blue = model bottom).

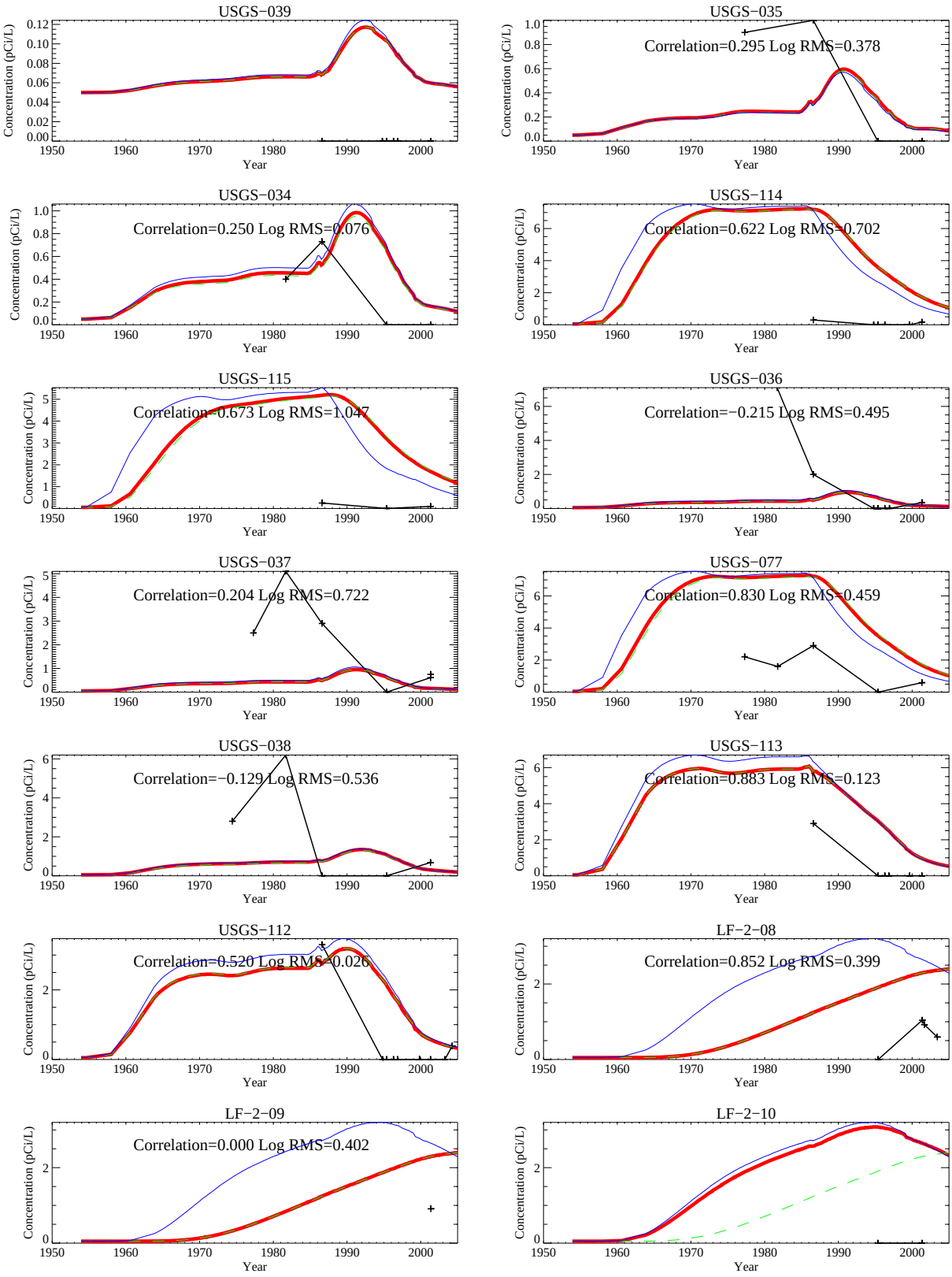

Figure A-8-30. Simulated and observed I-129 concentration histories (pCi/L) (measured = black crosses, thick red = model at screen center, dashed green = model top, blue = model bottom).

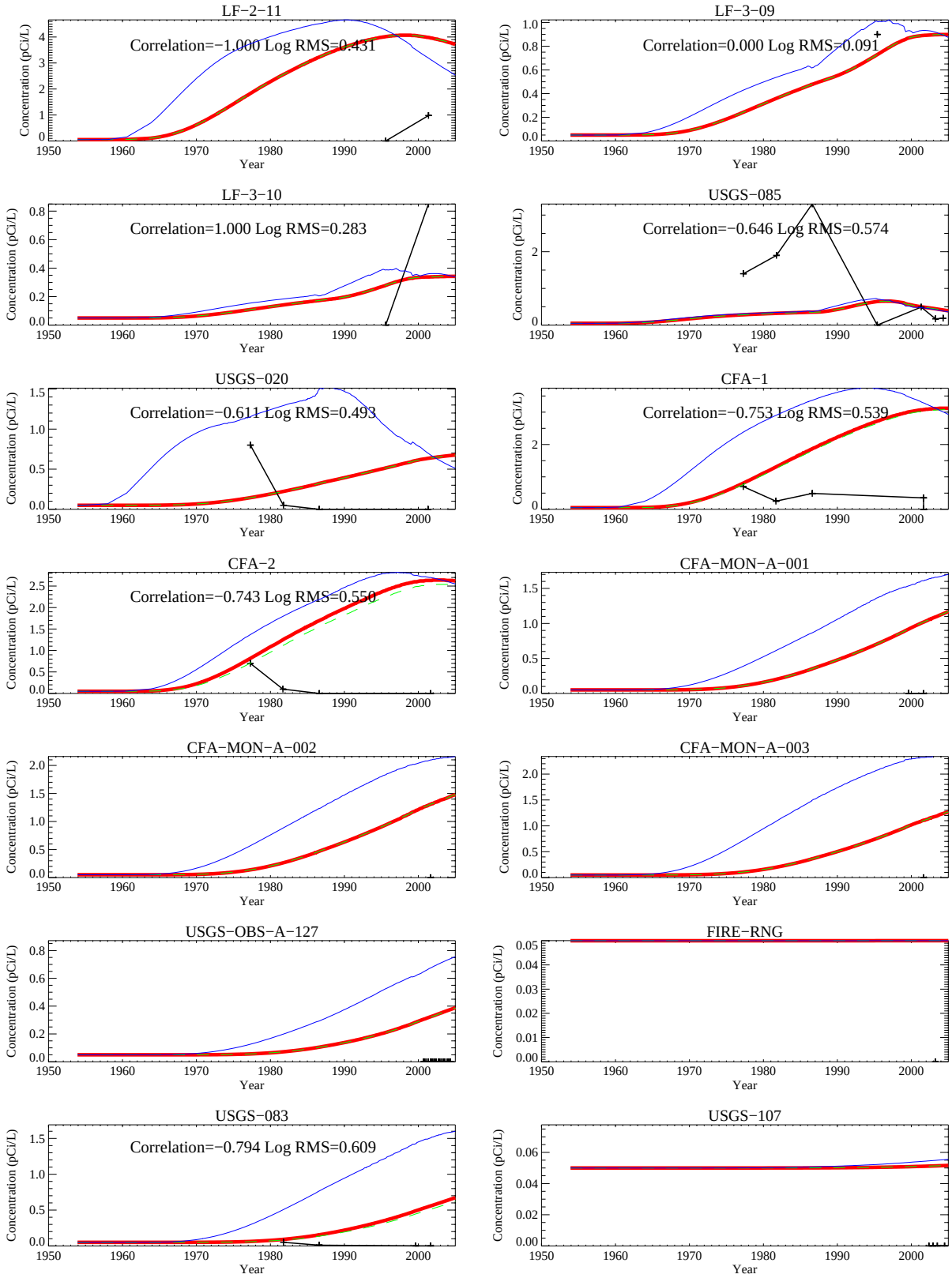

Figure A-8-31. Simulated and observed I-129 concentration histories (pCi/L) (measured = black crosses, thick red = model at screen center, dashed green = model top, blue = model bottom).

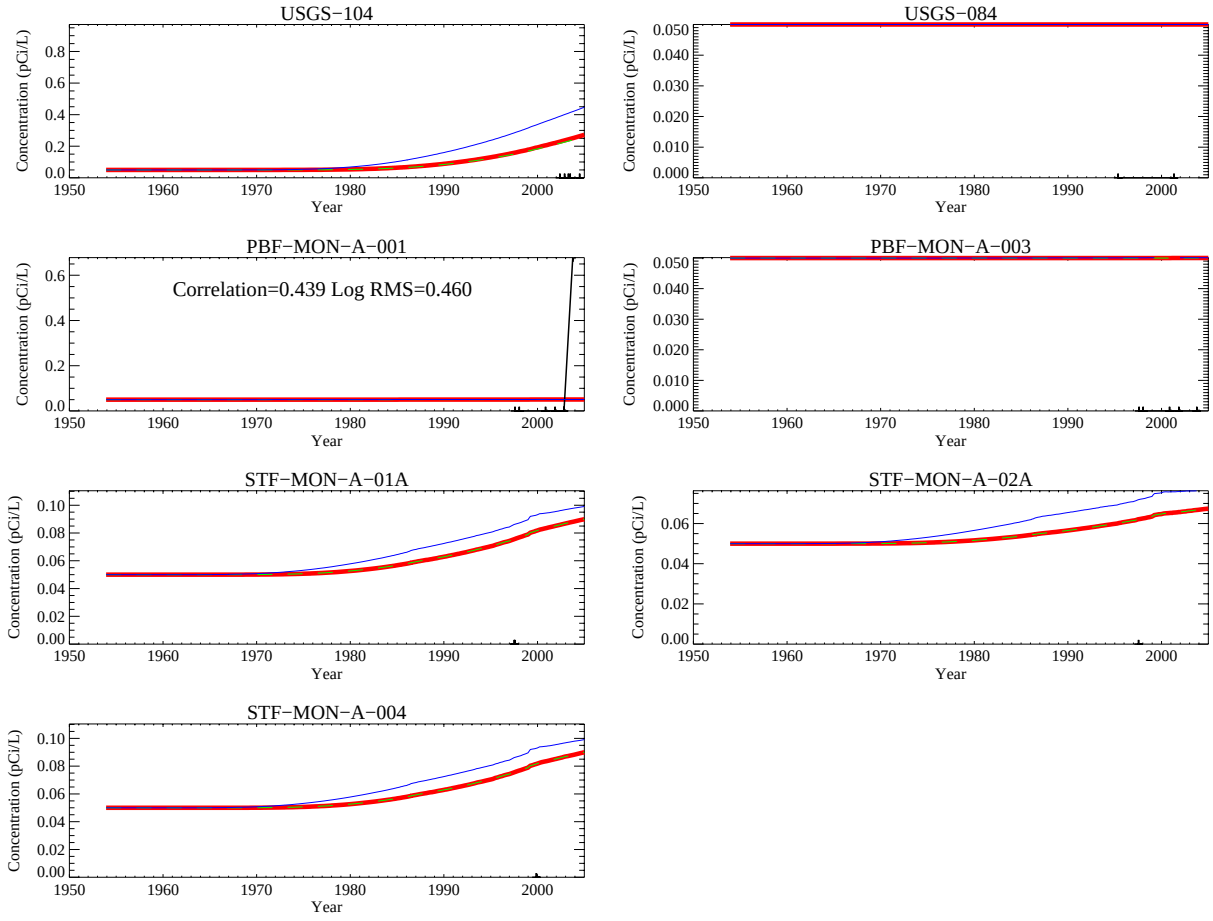

Figure A-8-32. Simulated and observed I-129 concentration histories (pCi/L) (measured = black crosses, thick red = model at screen center, dashed green = model top, blue = model bottom).

A-8.3.4 Nitrate in the Aquifer

The background concentration for nitrate is approximately 1.5-mg/L as N in the Snake River Plain Aquifer and surface waters near the INL Site (Orr et al. 1991). The simulated concentrations were adjusted to account for the background concentrations by adding this amount to the simulated value.

As with the I-129, the aquifer model was not calibrated to nitrate concentrations, but comparisons of predicted and observed data are presented. Service waste disposal records for nitrate were not kept, and the amounts used in these simulations were estimated based on discharge water volumes and average concentrations measured in 1981 (see Section A-5 of the main document). Field sampling for nitrate began during the mid-1990s in most of the aquifer wells, which is much later than the discharges in the injection well would have arrived at most downstream locations. Observed concentrations were assigned a zero value if the nitrate sample analysis was recorded as nondetect. These zero values should have been assigned the background concentration to be consistent with the upward adjustment of the simulation results by the background value. Overall, the model tends to overpredict nitrate concentrations, suggesting actual releases were smaller than the values used in these simulations. Figure A-8-33 illustrates the horizontal extent of the maximum concentration at any depth averaged over a 15-m well screen in 2004. Figures A-8-34 through A-8-36 illustrate the simulated and observed nitrate concentration history at each aquifer well with reported nitrate.

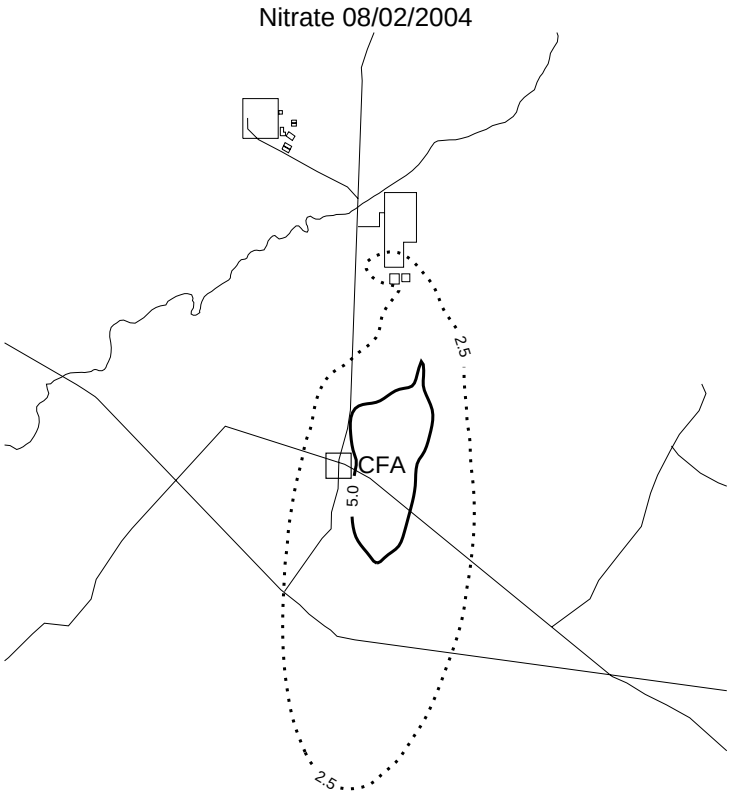

Figure A-8-33. Maximum simulated nitrate concentration (mg/L as N) in base grid averaged over a 15m well screen in 2004 (MCL=thick red line, 10*MCL=thin red line, MCL/5=thin black line, MCL/4=dashed black line).

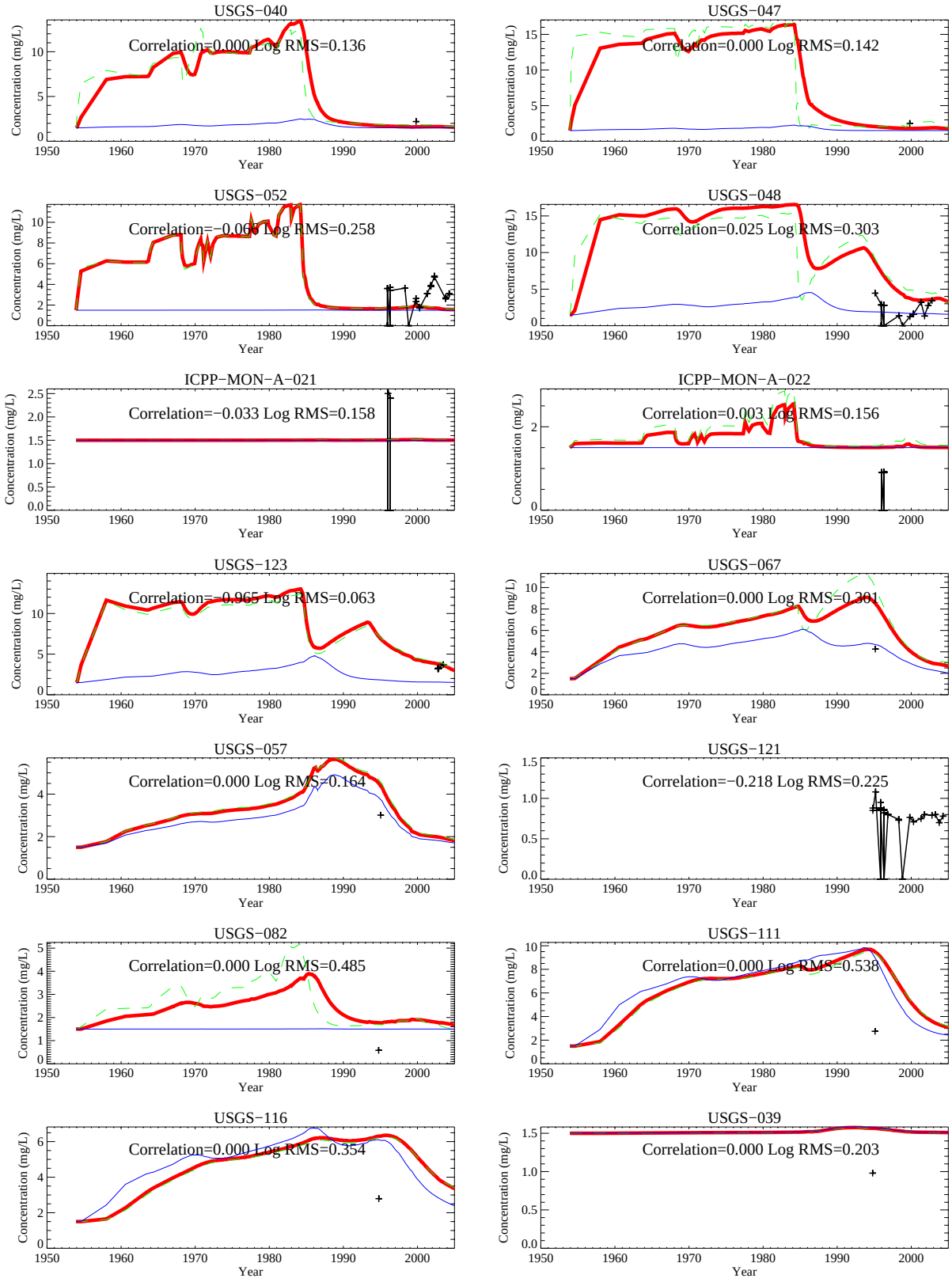

Figure A-8-34. Simulated and observed nitrate concentration histories (mg/L as N) (measured = black crosses, thick red = model at screen center, dashed green = model top, blue = model bottom).

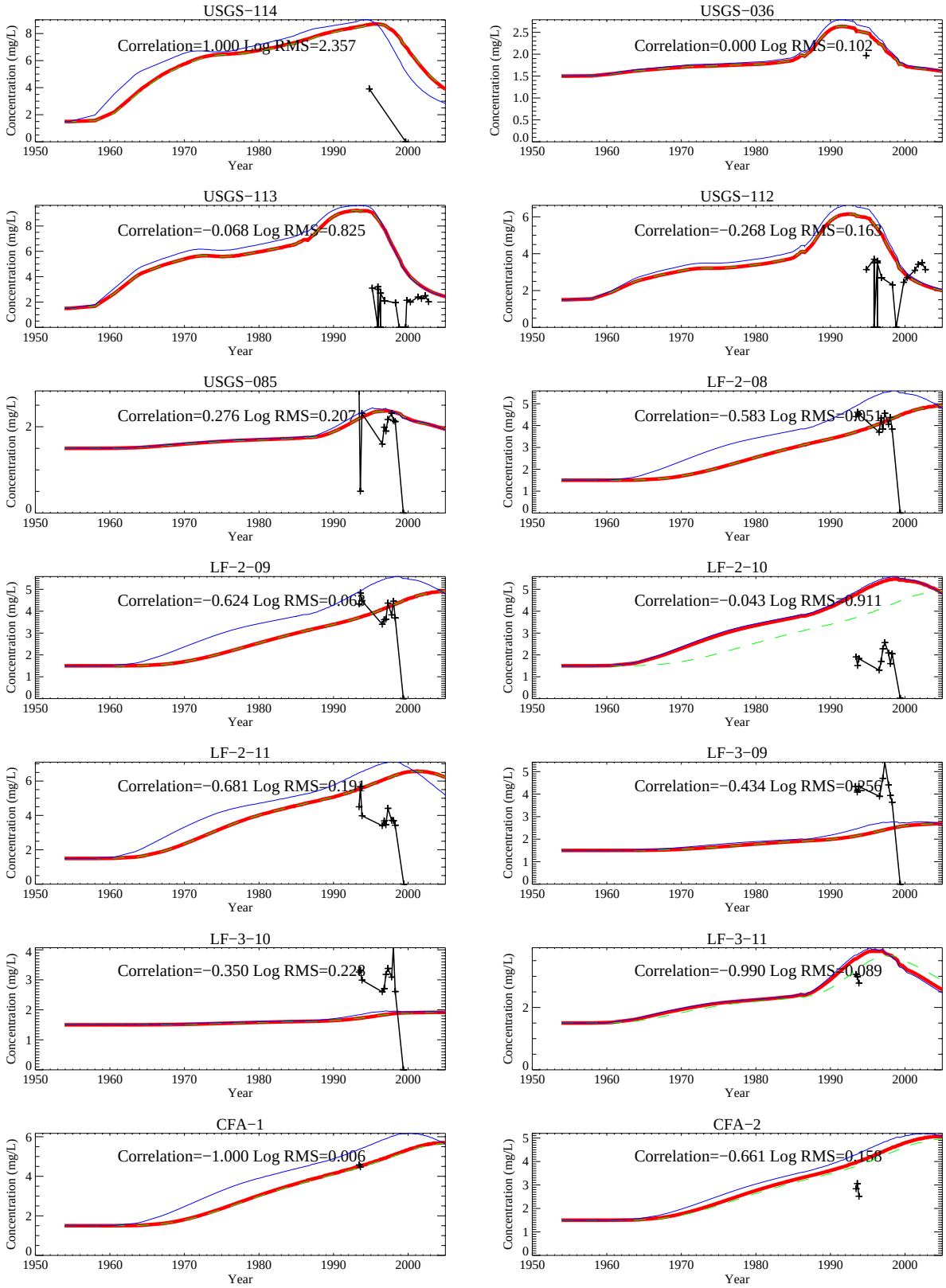

Figure A-8-35. Simulated and observed nitrate concentration histories (mg/L as N) (measured = black crosses, thick red = model at screen center, dashed green = model top, blue = model bottom).

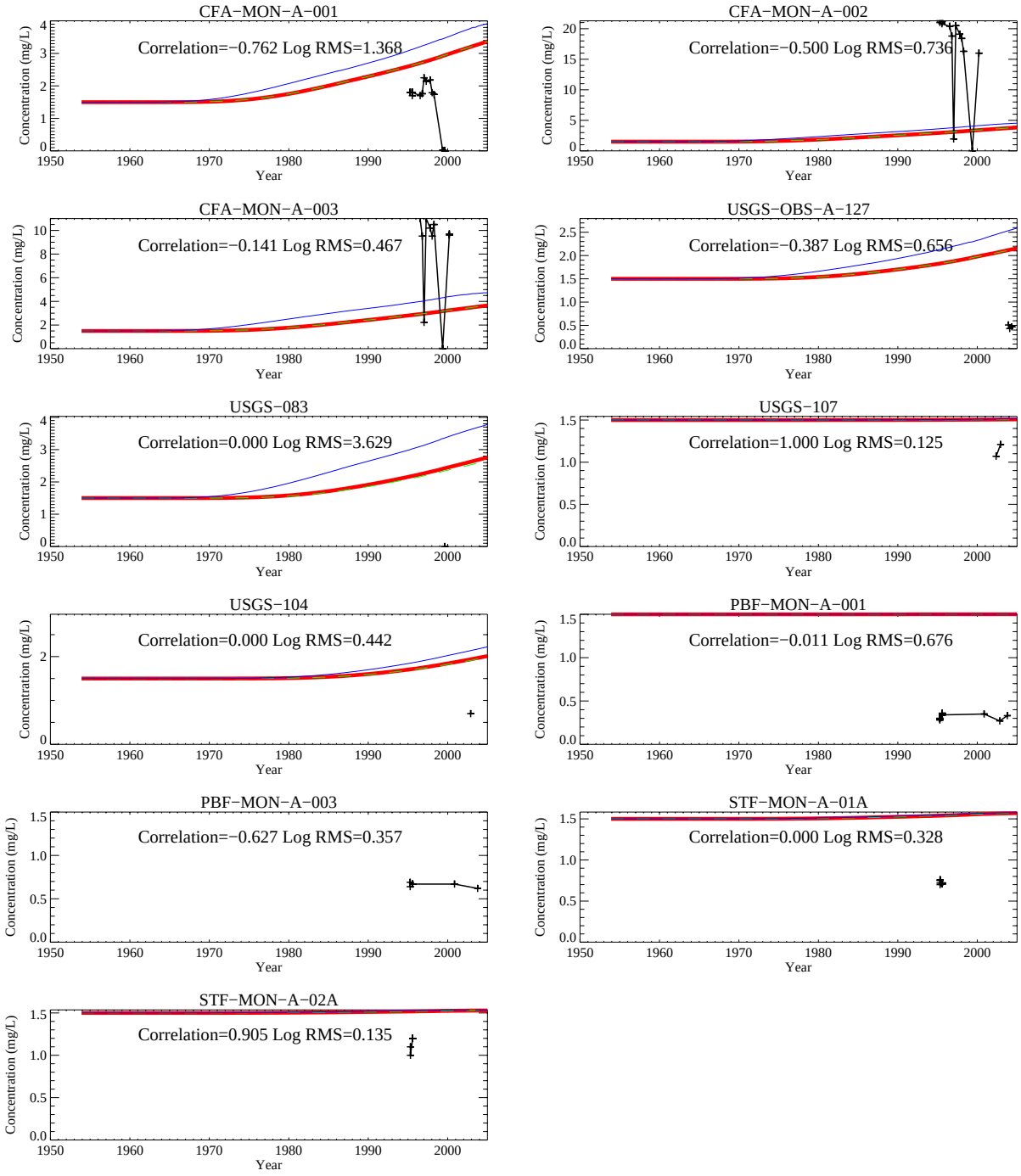

Figure A-8-36. Simulated and observed nitrate concentration histories (mg/L as N) (measured = black crosses, thick red = model at screen center, dashed green = model top, blue = model bottom).

A-8.3.5 Aquifer Flow Model Calibration Conclusions

The simulated large-scale aquifer gradient near the INTEC is southerly with a local eastern component below the INTEC facility footprint. This matches the large-scale regional gradient predicted in the summer 2004 water level measurements and is consistent with the small-scale flow directions observed in several INTEC aquifer wells from recent observations of colloid movement. The local eastern component may be due to a high-permeability zone running southeast under northern INTEC. The aquifer is relatively flat west of INTEC, and this is due to higher aquifer permeability in this area, which was confirmed by aquifer pump test data. The HI interbed may act as a weak dividing layer separating the contamination in the H and I basalt. The simulated and observed vertical concentrations suggest this is occurring. The large-scale aquifer gradient should keep the INTEC contamination east of the Subsurface Disposal Area.

A-8.3.6 Aquifer Transport Model Calibration Conclusions

The current tritium, Tc-99, I-129 and nitrate observed in the aquifer near INTEC are the result of vadose zone contaminant sources now reaching the aquifer. The CPP-3 injection well was closed in 1984 and the aquifer velocity between INTEC and the CFA is approximately 0.5 m/day.

The current model has better agreement with the observed tritium than with the other contaminants. This was because the tritium sources were well known and there was sufficient downgradient data to discern the arrival of specific peak concentrations. For these reasons, more emphasis was placed on matching the tritium data.

The current high Tc-99 concentrations occurring in the TF-Aquifer well could not be matched with either the vadose zone or aquifer models. The vadose zone model may be overestimating the attenuation occurring within the vadose zone or may have underestimated the vadose zone Tc-99 source term. The simulated concentrations seen in the vertical profile wells midway between INTEC and CFA matched the measured concentrations. This indicates dilution dispersion in the aquifer model was adequately parameterized because the source of the Tc-99 currently seen in these wells is from the CPP-3 injection well.

A-8.4 Summary of Aquifer Model Assumptions

The following list contains the primary assumptions used in developing the aquifer flow and transport models:

- The aquifer model domain is assumed to be fully saturated, and the response to pumping and recharge is assumed to behave as if confined. However, a transient water and contaminant flux is placed as an upper boundary condition.

- Production in the CPP-1, -2, and -4 wells is steady state.

- Injection in the CPP-3 well is transient.

- The Big Lost River loss rate between the INL Site diversion dam and the Lincoln Boulevard bridge gauging station represents the loss rate near INTEC, and quarterly averages adequately represent transient river recharge.

- The Big Lost River recharge prior to 1985 and after 2004 is steady state and is adequately represented by the long-term average between 1965 through 1987.

- Three material types (H basalt, HI interbed, and I basalt) and spatially varying H basalt permeability adequately represent aquifer heterogeneity.

- The observed isothermal temperature pofile with depth adequately denotes the thickness of the actively flowing portion of the aquifer.

- Flow in the fractured basalt was controlled by the fracture network and could be represented by a high-permeability, low-porosity equivalent porous medium.

- Water levels measured in summer 2004 are representative of the long-term natural gradient.

- All contaminant (except Site CPP-31 Sr-90 within the alluvium) sorption processes can be lumped into a single contaminant-specific soil/water distribution coefficient (K_d) parameter.

- There is sufficient accuracy in the contaminant source terms and sufficient number of concentration observations for aquifer flow model calibration.

- The aquifer model can be linked to the vadose zone model through a transient water and contaminant flux.

- There is no gaseous-phase contaminant transport to the aquifer.

A-9 GROUNDWATER PATHWAY RISK PREDICTION

In this section, predictions of the future baseline groundwater concentrations are presented. In view of the large number of COPCs, a screening analysis was performed to reduce the number of contaminants incorporated into the full 3-D vadose zone and aquifer models. The screening analysis used very simple, but conservative assumptions. The screening analysis procedure and results are presented in Section A-9.1. The contaminant source terms used in the modeling are presented in Section A-9.2, and the simulation results are presented in Section A-9.3.

A-9.1 Screening Analysis

An extensive screening of groundwater COPCs was performed in the OU 3-13 RI/BRA (DOE-1997). The OU 3-13 COPC list was used as the starting point for the OU 3-14 screening process. The list was reviewed using process knowledge and new data collected since the OU 3-13 RI/BRA to determine if any additional COPCs from the OU 3-14 tank farm sites needed to be added to this list. As a result of the review, nitrate and C-14 were added to the list of COPCs. C-14 was added to the list of COPCs because it is an activation product in spent nuclear fuel.

All of the OU 3-14 alluvium samples collected in 2004 were analyzed for C-14. All sample results were nondetect except for the duplicate sample collected from the 36-40-ft depth in CPP-31 (the primary sample was nondetect and the duplicate was 3 pCi/g). Tank farm waste has been analyzed for C-14, but it has never been detected. The ORIGEN code was used to predict the ratio of C-14 to Cs-137 in the fuel and it is approximately 10^{-9} (see Table A-9-1). The C-14 in the waste is likely much lower than in the fuel because it would be oxidized and released as CO_2 during the fuel dissolution process. INTEC perched water and Snake River Plain Aquifer samples have been analyzed for C-14. The maximum C-14 concentrations measured in the Snake River Plain Aquifer in 2004 were less than 1% of the Snake River Plain Aquifer MCL. The maximum C-14 measured in the perched water in 2004 was approximately 4% of the Snake River Plain Aquifer MCL. Although C-14 was not expected to be a final COC for the tank farm soils and groundwater, it was part of the groundwater COPC screening because it had not been part of the previous screening conducted in OU 3-13.

All of the OU 3-14 COPCs were then evaluated using the GWSCREEN model (Rood 1999) and conservative parameters. The initial list of COPCs and screening results are provided in Table A-9-2. The GWSCREEN model was developed to address CERCLA sites at the INL Site. The code, coupled with a set of default parameter values identified in the CERCLA Track 2 risk assessment process (DOE-ID 1994), provides conservative estimates of groundwater concentrations and ingestion doses at the INL Site.

The GWSCREEN conceptual model is illustrated in Figure A-9-1. Contaminants are mixed homogeneously with an assumed volume of soil. One-dimensional transport in the unsaturated zone is assumed. The dimensions of the source were assumed to be $100 \times 100 \times 0.5$ m. The horizontal dimensions are based on the minimum area of the computational blocks used in the TETRAD model. The thickness of the contaminated zone (0.5 m) was based on guidance in the National Council on Radiation Protection (NCRP) Report Number 123, *Screening Models for Releases of Radionuclides* (NCRP 1996).

The subsurface environment beneath the INL Site is composed of basalt flows separated by sedimentary interbeds. The basalt flows are oftentimes fractured, allowing water to move freely in the vertical direction. The Track 2 methodology (DOE-ID 1994) recognized this feature of the system and assumed water transport time through the fractured basalt is relatively instantaneous. Water travel time through the entire unsaturated zone is ultimately controlled by the presence of sedimentary interbeds. Therefore, only transport through sedimentary interbeds was considered when computing contaminant transport in the unsaturated zone. The total thickness of sedimentary interbeds was obtained from the geologic model of INTEC and represents the total interbed thickness below CPP-31 (17.6 m). Most of the contamination at INTEC was derived from leaky pipes at CPP-31; therefore, the sedimentary interbeds present below this facility would be most relevant in terms of estimating contaminant transport in the unsaturated zone.

Infiltration of precipitation through the alluvium was estimated to be 18 cm/yr across the INTEC site. This value is substantially greater than the Track 2 default value of 10 cm/yr (DOE-ID 1994) because much of INTEC is unvegetated gravely alluvium. Additional anthropogenic water from leaky pipes was estimated to increase the infiltration through surface alluvium from 18 cm/yr to 40 cm/yr.

Water fluxes through sedimentary interbeds at INTEC are influenced by the presence of the Big Lost River and the INTEC percolation ponds. Annual average water fluxes through interbeds in the north end of INTEC (near CPP-31) were estimated to be ~2 m/yr. The value of 2 m/yr was used in the GWSCREEN simulation to estimate water travel time through the interbeds. The GWSCREEN code only allows input of a single water flux. Therefore, a water flux of 2 m/yr was input and source thickness was adjusted so that leaching from the alluvium would occur at a rate equivalent to 40 cm/yr infiltration. The leach rate constant is given by

$$\lambda_L = \frac{I}{H\,\theta\left(1+\frac{K_d\rho}{\theta}\right)} \qquad \text{(A-9-1)}$$

where

I = assumed infiltration rate (0.18 m yr^{-1})

H = assumed waste thickness (0.5 m)

ρ = bulk density (g/cm^3)

K_d = sorption coefficient (g/cm^3)

θ = moisture content (m^3/m^3).

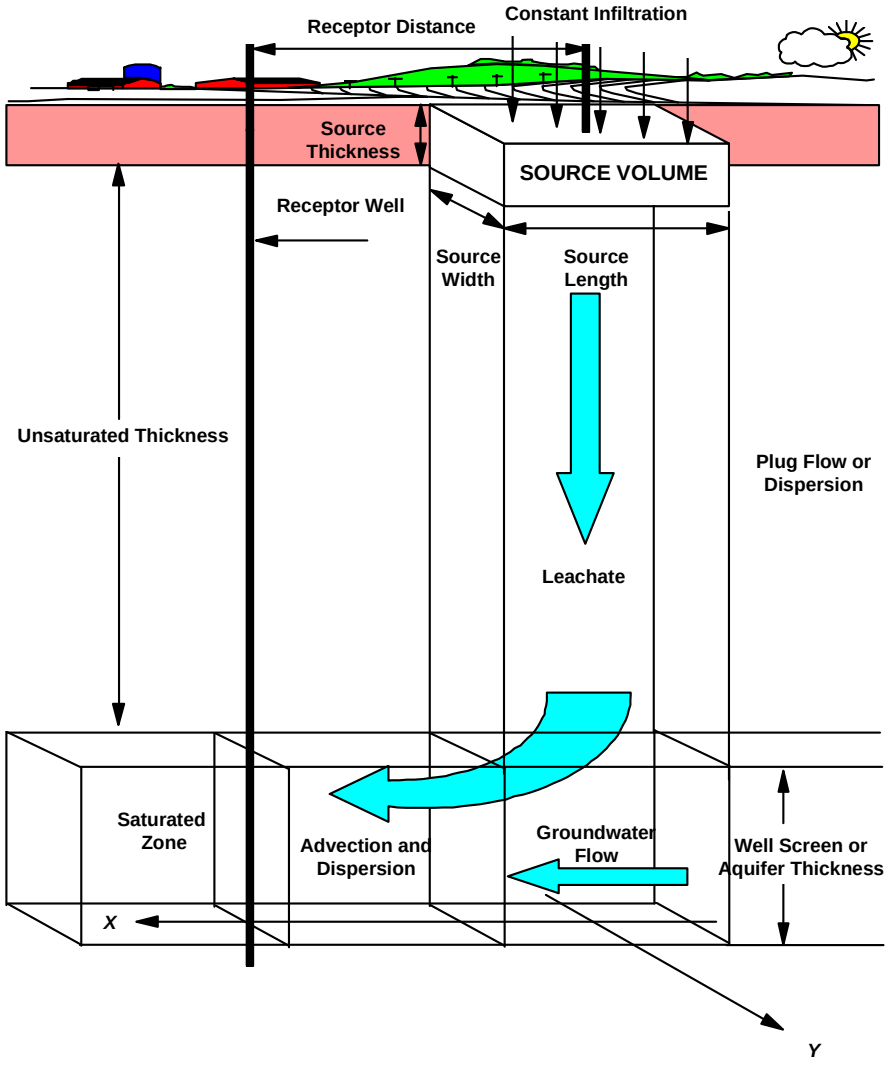

Figure A-9-1. Conceptual model for GWSCREEN.

The equivalent source thickness can be calculated by rearrangement of Equation 9-1.

$$H = \frac{I}{\lambda_L \, \theta \left(1 + \frac{K_d \rho}{\theta}\right)} \tag{A-9-2}$$

The moisture content in the sources was determined using the van Genuchten fitting parameters for high-permeability alluvium (α = 127 1/m. n = 1.1, K_{sat} = 4170, θ_{sat} = 0.42, θ_r = 0.0002). Using the van Genuchten parameters for high-permeability alluvium and the stated infiltration rates of 40 cm/yr for the alluvium and 2 m/yr for the interbeds resulted in moisture contents of 0.343 and 0.367 respectively. The leach rate constant for 40 cm/yr infiltration (assuming a K_d of zero) is

$$\lambda_L = \frac{40\,\text{cm/yr}}{0.5\,\text{m}\ \ 0.343} = 2.33\,\text{yr}^{-1} \tag{A-9-3}$$

The effective source thickness is then

$$H = \frac{2\,\text{m/yr}}{2.33\,\text{yr}^{-1}\,0.367} = 2.34\,\text{m} \qquad \text{(A-9-4)}$$

Dispersion was considered in the unsaturated zone because dispersion is a conservative assumption when contaminants with short half-lives relative to their transit times are considered. Contaminants entering the aquifer from the unsaturated zone mix with water in the aquifer over a depth defined by a typical well screen of 15 m (DOE-ID 1994). Concentrations are then evaluated at the downgradient edge of the source. This receptor is the point where the highest concentrations in the aquifer are computed.

The GWSCREEN model also considers transport of radioactive progeny. For simplicity, progeny are assumed to travel at the same rate as their parent. Under most circumstances, this assumption leads to conservative dose estimates at the receptor point. However, when considering the transport of a short-lived immobile parent that has a long-lived mobile progeny, results can be distorted and, in many cases, not conservative. This situation occurs for the Pu-241⇒Am-241⇒Np-237 and Pu-238⇒U-234 decay chains. In general, the short-lived immobile parent nuclide never leaves the waste zone and instead decays to its more mobile long-lived progeny. The sorption characteristics of the progeny then determine the overall transit time of the decay chain along with accompanying radiation dose. For conservatism, the entire activity of the short-lived immobile parent is converted to the equivalent mobile progeny activity by:

$$A_{Prog} = A_{Parent}\,\frac{T_{parent}}{T_{Prog}} \qquad \text{(A-9-5)}$$

where

A_{Prog} = equivalent activity of the long-lived mobile progeny (Ci)
A_{Parent} = original activity of the short-lived immobile parent (Ci)
T_{Prog} = half-life of the long-lived mobile progeny (years)
T_{Parent} = half-life of the short-lived immobile parent (years).

The receptor scenario assumes the person drinks 2 L of water per day for 365 days per year. Ingestion doses are computed using dose conversion factors published in EPA (1988) and include contributions from all progeny.

The screening criterion for radionuclides was set at 0.4 mrem/yr and was based on 1/10th the allowable drinking water dose for beta-gamma-emitting radionuclides of 4 mrem/yr as stated in 40 CFR 141. This was the same screening criterion that was applied in the Idaho CERCLA Disposal Facility (ICDF) Performance Assessment (DOE-ID 2003c). For metals, maximum groundwater concentrations were compared with their corresponding maximum contaminant limits (Snake River Plain Aquifer MCLs). Uranium was addressed both as a radionuclide and a metal.

Input data for the GWSCREEN screening simulation (Figure A-9-1) were primarily obtained from the Track 2 guidance document (DOE-ID 1994) and modified as noted. The receptor well is placed on the downgradient edge of the source. Note that the receptor distance is measured from the center of the source. The conceptual model assumes no presence of engineered barriers or other devices that would limit infiltration and reduce contaminant leaching. The waste is then assumed to be exposed to infiltrating water, and contaminants are leached from the waste and move into the subsurface.

Table A-9-1 Parameter values for the GWSCREEN screening analysis.

Parameter	Value	Reference
Length parallel to groundwater flow	100 m	TETRAD large-scale vadose zone model grid cell size
Width perpendicular to groundwater flow	100 m	TETRAD large-scale vadose zone model grid cell size
Infiltration through alluvium	0.40 m/yr	This study
Thickness of source	0.5 m	Based on default groundwater scenario in NCRP (1996)
Water-filled porosity – source	0.343	This study (high-permeability alluvium and 40 cm/yr infiltration
Water-filled porosity – unsaturated zone	0.4438	This study (high-permeability interbed and 2 m/yr infiltration)
Unsaturated interbed thickness (transport time through basalt assumed to be instantaneous)	17.6 m	Interbed thickness below CPP-31
Bulk density-source	1.5 g/cm^3	DOE-ID (1994)
Bulk density-unsaturated zone	1.9 g/cm^3	DOE-ID (1994)
Bulk density-saturated zone	1.9 g/cm^3	DOE-ID (1994)
Well screen thickness[a]	15 m	DOE-ID (1994)
Receptor distance parallel to groundwater flow (measured from center of source)	50 m	Based on guidance in DOE-ID (1994)
Receptor distance perpendicular to groundwater flow (measured from center of source)	0 m	Based on guidance in DOE-ID (1994)
Water ingestion rates for receptor	2 L/d	DOE-ID (1994)
Exposure frequency	365 d/yr	DOE-ID (1994)
Darcy velocity in aquifer	21.9 m/yr	Fate and transport modeling design of the ICDF landfill cap (DOE-ID 2003d; EDF-ER-275)
Longitudinal dispersivity	9 m	DOE-ID (1994)
Transverse dispersivity	4 m	DOE-ID (1994)
Aquifer porosity	0.03	DOE-ID (2003d)
a. A vertically averaged solution is used per Track 2 guidance (DOE-ID 1994). Thickness of the vertical section is taken to be the well screen thickness.		

Nuclide-specific data are reported in Table A-9-2. The primary source of sorption coefficient data was DOE-ID (1994) (the Track 2 screening process). If a value for a given nuclide did not exist in DOE-ID (1994), then other sources were consulted, including Sheppard and Thibault (1990), NCRP (1996), and DOE-ID (1997). The sorption coefficients or K_d values were assumed to be applicable to sedimentary rocks and materials that make up the surface alluvium and interbeds. Sorption coefficients in fractured basalt, which makes up most of the aquifer, tend to be lower than in sedimentary materials because surface area of available sorption sites are lacking. The ratio of the aquifer basalt-to-soil K_d value was estimated in the INTEC RI/BRA (DOE-ID 1997) to be 0.04. The ratio was multiplied by all sediment K_d values to obtain the aquifer K_d values used in the GWSCREEN simulation. Radionuclide solubility was assumed to be infinite in all cases. The Darcy velocity in the aquifer was taken from the screening analysis for the ICDF PA (DOE-ID 2003c).

A-9.1.1 Results of GWSCREEN Analysis

Screening results are given in Table A-9-2 where the initial 22 radionuclides and their daughter products are listed in the first column. The last column indicates the 14 nuclides that were removed from further consideration. The last column also indicates the 8 remaining radionuclides that were carried forward based on the 0.4-mrem criteria. These remaining nuclides include H-3, I-129, Np-237, Pu-239, Pu-240, Sr-90, Tc-99, and U-234.

Uranium isotopes were compared with the Snake River Plain Aquifer MCL of 30 µg/L (Table A-9-3). Each uranium isotope represents a different uranium mass because each isotope has a different half-life. Therefore, the 30-µg/L limit was converted to an equivalent activity concentration for each uranium isotope and compared with the maximum activity concentration estimated by GWSCREEN for that isotope. The sum of the ratio of the maximum uranium isotope concentration to the isotope-specific Snake River Plain Aquifer MCL activity concentration provides a measure of the total uranium concentration in groundwater. If the aforementioned ratio is less than one, then the total uranium mass is less than 30 µg/L. In this screening exercise, none of the uranium isotope mass concentrations exceeded the Snake River Plain Aquifer MCL and the total uranium mass concentration was less than the Snake River Plain Aquifer MCL.

Evaluation of metals was limited to mercury, arsenic, chromium, and nitrate. Water solubilities were obtained from Perry et al. (1984), except for nitrate, which assumed an infinite solubility. All nonradionuclide concentrations were less than their respective Snake River Plain Aquifer MCLs except nitrate, which had a maximum concentration about nine times the Snake River Plain Aquifer MCL of 10 mg/L. The results of the nonradionuclide screening are provided in Table A-9-4.

The screening analysis used the Track 2 guidance K_d values (DOE-ID 1994) and was performed prior to the estimation of the groundwater K_d values used for the RI/BRA full modeling process. The Track 2 K_d values are generally very conservative, but several RI/BRA K_d values were smaller than those used in the screening analysis. These contaminants included: Am-241, Arsenic, C-14, Chromium, Cs-137, Np-237, Sr-90 and U-235. The RI/BRA analysis evaluated the risk from Np-237, Sr-90 and U-235; and the effect of a less conservative K_d was considered. The remaining contaminants with screening K_d values larger than the RI/BRA values all had screening concentrations several orders of magnitude lower than the SRPA MCL and would not pose a risk to the SRPA, if the RI/BRA values were used in the screening analysis.

Table A-9-2 Results of radionuclide screening (blue color denotes the parent contaminants are retained for the full modeling process)

Radionuclide Progeny[a]	Mass	Half-Life (Years)	Activity (Ci)	Ingestion DCF (rem/Ci)	K_d (mL/g)	Dose (mrem)	Is Dose < 0.4 (mrem)?
Am-241 (Np-237)	237	2.14E+06	4.10E-04	4.44E+06	8	1.4E-01	
U-233	233	1.59E+05		2.89E+05	6	7.4E-06	
Th-229	229	7.43E+03		4.03E+06	100	4.1E-08	
TOTAL						1.4E-01	Yes
C-14	14	5,730	2.81E-05	2,086.8	5	8.3E-06	Yes
Co-60	60	5.27E+00	1.96E+01	2.69E+04	10	5.6E-04	Yes
Cs-137	137	3.02E+01	1.91E+04	5.00E+04	500	1.9E-15	Yes
H-3	3	1.23E+01	9.71E+00	6.40E+01	0	1.6E+00	NO
I-129	129	1.57E+07	1.26E-03	2.76E+05	0	1.1E+00	NO
Np-237	237	2.14E+06	2.72E-02	4.44E+06	8	9.6E+00	
U-233	233	1.59E+05		2.89E+05	6	4.9E-04	
Th-229	229	7.43E+03		4.03E+06	100	2.7E-06	
TOTAL						9.6E+00	NO
Pu-236 (U-232)	232	7.20E+01	2.13E-05	1.31E+06	6	1.4E-03	
Th-228	228	1.91E+00		8.08E+05	100	5.2E-05	
TOTAL						1.4E-03	Yes
Pu-238 (U-234)	234	2.45E+05	6.71E-03	2.83E+05	6	2.1E-01	
Th-230	230	7.54E+04		5.48E+05	100	2.4E-05	
Ra-226	226	1.60E+03		1.33E+06	100	1.1E-06	
Pb-210	210	2.20E+01		7.27E+06	100	3.6E-06	
TOTAL						2.1E-01	Yes
Pu-239	239	2.41E+04	6.94E+00	3.54E+06	22	9.9E+02	
U-235	235	7.04E+08		2.67E+05	6	7.0E-05	
Pa-231	231	3.28E+04		1.06E+07	550	1.3E-07	
Ac-227	227	2.18E+01		1.48E+07	450	1.8E-07	
TOTAL						9.9E+02	NO
Pu-240	240	6.57E+03	1.07E+00	3.54E+06	22	1.5E+02	
U-236	236	2.34E+07		2.69E+05	6	3.2E-04	

Radionuclide Progeny[a]	Mass	Half-Life (Years)	Activity (Ci)	Ingestion DCF (rem/Ci)	K_d (mL/g)	Dose (mrem)	Is Dose < 0.4 (mrem)?
Th-232	232	1.41E+10		2.73E+06	100	2.0E-12	
Ra-228	228	5.75E+00		1.44E+06	100	8.0E-13	
Th-228	228	1.91E+00		8.08E+05	100	4.9E-13	
TOTAL						1.5E+02	NO
Pu-241 (Np-237)	241	2.14E+06	4.88E-04	4.44E+06	8	1.7E-01	
U-233	233	1.59E+05		2.89E+05	6	8.9E-06	
Th-229	229	7.43E+03		4.03E+06	100	4.9E-08	
TOTAL						1.7E-01	Yes
Pu-242	242	3.76E+05	1.73E-04	3.36E+06	22	2.4E-08	
U-238	238	4.47E+09		2.70E+05	6	2.5E-10	
U-234	234	2.45E+05		2.83E+05	6	1.4E-13	
Th-230	230	7.54E+04		5.48E+05	100	2.0E-17	
Ra-226	226	1.60E+03		1.33E+06	100	1.5E-18	
Pb-210	210	2.20E+01		7.27E+06	100	6.7E-18	
TOTAL						2.5E-08	Yes
Pu-244	244	8.26E+07	1.80E-11	4.03E+08	100	4.4E-10	
Pu-240	240	6.57E+03		3.54E+06	22	4.0E-10	
U-236	236	2.34E+07		2.69E+05	6	1.9E-15	
Th-232	232	1.41E+10		2.73E+06	100	3.6E-23	
Ra-228	228	5.75E+00		1.44E+06	100	1.5E-23	
Th-228	228	1.91E+00		8.08E+05	100	9.6E-24	
TOTAL						8.4E-10	Yes
Sr-90	90	2.86E+01	1.81E+04	1.42E+05	12	3.9E+03	NO
Tc-99	99	2.13E+05	3.56E+00	1.46E+03	0.2	7.9E+00	NO
U-232	232	7.20E+01	2.78E-05	1.31E+06	6	1.8E-03	
Th-228	228	1.91E+00		8.08E+05	100	6.8E-05	
TOTAL						1.9E-03	Yes
U-233	233	1.59E+05	2.61E-06	2.89E+05	6	8.4E-05	
Th-229	228	5.75E+00		4.03E+06	100	2.4E-05	

Radionuclide Progeny[a]	Mass	Half-Life (Years)	Activity (Ci)	Ingestion DCF (rem/Ci)	K_d (mL/g)	Dose (mrem)	Is Dose < 0.4 (mrem)?
TOTAL						1.1E-04	Yes
U-234	234	2.44E+05	4.36E-02	2.83E+05	6	1.4E+00	
Th-230	230	7.54E+04		5.48E+05	100	1.6E-04	
Ra-226	226	1.60E+03		1.33E+06	100	6.9E-06	
Pb-210	210	2.20E+01		7.27E+06	100	2.3E-05	
TOTAL						1.4E+00	NO
U-235	235	7.04E+08	6.04E-03	2.67E+05	6	1.8E-01	
Pa-231	231	3.28E+04		1.06E+07	550	1.9E-04	
Ac-227	227	2.18E+01		1.48E+07	450	2.2E-04	
TOTAL						1.8E-01	Yes
U-236	236	2.34E+07	4.47E-03	2.69E+05	6	1.3E-01	
Th-232	232	1.41E+10		2.73E+06	100	4.6E-10	
Ra-228	228	5.75E+00		1.44E+06	100	1.8E-10	
Th-228	228	1.91E+00		8.08E+05	100	1.1E-10	
TOTAL						1.3E-01	Yes
U-238	238	4.47E+09	6.33E-04	2.70E+05	6	1.7E-02	
U-234	234	2.45E+05		2.83E+05	6	5.5E-06	
Th-230	230	7.54E+04		5.48E+05	100	3.2E-10	
Ra-226	226	1.60E+03		1.33E+06	100	9.4E-12	
Pb-210	210	2.20E+01		7.27E+06	100	2.7E-11	
TOTAL						1.7E-02	Yes

a. Progeny are left justified in this column. Radionuclides in parentheses indicate the progeny that is simulated. The activity inventory represents that of the parent converted to equivalent progeny.

Table A-9-3 Uranium isotope mass concentrations and comparison to the Snake River Plain Aquifer MCL of 30 µg/L.

Uranium Isotope	Specific Activity (Ci/g)	Equivalent SRPA MCL Activity Concentration (pCi/L)	Maximum Concentration (pCi/L)	Ratio to SRPA MCL
U-232	2.24E+01	6.72E+08	1.9E-03	2.81E-12
U-233	9.64E-03	2.89E+05	4.3E-04	1.48E-09
U-234	6.23E-03	1.87E+05	7.1E+00	3.82E-05
U-235	1.92E-06	5.77E+01	9.9E-01	1.72E-02
U-236	6.51E-05	1.95E+03	7.3E-01	3.75E-04
U-238	3.33E-07	9.99E+00	1.0E-01	1.04E-02
TOTAL				2.80E-02

Table A-9-4 Results of nonradionuclide screening.

Non-radionuclide	Mass	Inventory (mg)	SRPA MCL (mg/L)	K_d (mL/g)	Water Solubility (mg/L)	Peak Concentration (mg/L)	Ratio to SRPA MCL
Hg	2.006E+02	7.164E+07	2.00E-03	100	7	7.30E-04	3.65E-01
Cr	5.200E+01	1.309E+07	1.00E-01	30	1,740,000	4.43E-04	4.43E-03
As	7.492E+01	4.315E+03	5.00E-03	50	658,000	8.78E-08	1.76E-05
NO_3	6.200E+01	2.116E+10	1.00E+01	0	∞	9.23E+01	9.23E+00

A-9.2 Contaminants of Potential Concern Source Terms

The results of the screening analysis identified 10 COPCs which were simulated with the vadose zone and aquifer models. The simulated radionuclide COPCs were the following: H-3, I-129, Np-237, Pu-239, Pu-240, Sr-90, Tc-99, and U-234. The nonradionuclides were mercury and nitrate. The simulations included the following contaminant sources: (1) the known OU 3-14 releases, (2) the known OU 3-13 liquid releases, (3) the OU 3-13 soil sources, (4) the CPP-3 injection well releases, and (5) the former percolation pond releases. The source term placement within the model is the same as that presented in Section A-5.1.4.1.

The contaminants originating at RTC were not included in the OU 3-14 analysis because the current aquifer model predicts those contaminants to remain mostly west of the INTEC plume. The two plumes may merge far south and west of the INTEC, but the contaminant concentrations in the areas where the two plumes may intersect are very dilute. The OU 3-14 release sources are summarized in Section A-9.2.1. The OU 3-13 soil contamination sources are presented in Section A-9.2.2, and the service waste sources (CPP-3 injection well and former percolation ponds) are presented in Section A-9.2.3. These source inventories are summarized in Table A-9-5.

Table A-9-5 COPC source term summary.

COPC	OU 3-14 Releases (Ci or kg)	Injection Well (Ci or kg)	Former Percolation Ponds (Ci or kg)	OU 3-13 Contaminated Soil Sites (Ci or kg)	OU 3-13 Liquid Releases (Ci)	Total (Ci or kg)
H-3	9.71	2.01e+4	9.99e+2	0.	378.1	2.15e+4
I-129	1.26e-3	0.86	8.2e-2	3.89e-2	0.	.982
Np-237	2.72e-2	1.07	0.	1.33e-1	0.	1.23
Pu-239	6.94	1.35e-2	1.14e-3	1.05e+0	0.	8.01
Pu-240	1.07	6.77e-3	5.71e-4	1.18e-1	0.	1.19
Sr-90	1.81e+4	2.43e+1	2.95e-1	9.18e+2	308.8	1.94e+4
Tc-99	3.56	1.19e+1	1.13e+0	9.30e-2	0.	16.7
U-234	0.138[a]	1.35e-1	4.03e-2	1.40e-1	0.	.410
Mercury	72.4	4.00e+2	0.	5.85e+2	0.	1.06e+3
Nitrate	2.12e+4	2.83e+6	1.31e+6	0.	0.	4.16e+6

a. Early estimate of U-234 source term. The estimate for U-234 developed in Section 5 of the main document was smaller, but the model was not rerun with the latest value because the source term was conservatively larger.

A-9.2.1 Release Estimates for OU 3-14 Sites

Based on process knowledge, some of the release estimates used for the OU 3-13 RI/FS were determined to be inaccurate. Because of their importance, the release times, concentrations, and volumes were revised based on an in-depth analysis of INTEC operations. In some cases (e.g., CPP-31), the total volumes were increased; others were decreased. A complete discussion of the revision process and rationale can be found in Section 5 of the main document. Each of the contaminant sources contained in Table A-9-6 were incorporated into the model as a liquid release during the estimated release period.

Table A-9-6 OU 3-14 liquid releases.

Site	First Day	Last Day	Liquid Volume (gal)	H-3 (Ci)	I-129 (Ci)	Np-237 (Ci)	Pu-239 (Ci)	Pu-240 (Ci)	Sr-90 (Ci)	Tc-99 (Ci)	U-234 (Ci)	Nitrate (kg)	Mercury (kg)
CPP-31	11/1/72	11/7/72	18,600	2.34E+0	2.51E-4	2.51E-2	4.34E+0	1.00E+0	1.59E+4	3.17E+00	4.34E-2	19,100	70.1
CPP-28	2/1/74	4/30/74	230.	5.59E-1	1.52E-4	5.80E-6	2.97E-2	1.04E-2	6.62E+2	1.10E-1	8.28E-6	130	0.518
CPP-79 deep1967	1/1/67	1/1/67	120.	1.58E+0	1.07E-4	3.67E-4	7.33E-1	6.77E-3	2.62E+2	4.51E-2	1.49E-5	114	0.092
CPP-79 deep1973	1/1/73	1/2/73	280.	3.68E+0	2.50E-4	8.55E-4	1.71E+0	1.58E-2	6.12E+2	1.05E-1	3.49E-5	266	0.214
CPP-27/33 1964 scrub solution	1/1/64	12/31/64	180.	4.00E-1	1.10E-4	2.99E-4	4.08E-2	1.09E-2	2.40E+2	4.00E-2	3.50E-5	0	0.478
CPP-27/33 1966-1967 scrub solution	1/1/66	12/31/67	360.	8.00E-1	2.20E-4	5.99E-4	8.17E-2	2.18E-2	4.80E+2	8.00E-2	7.00E-5	0	0.957
CPP-27/33 1964-1974 decon solution	1/1/64	12/31/73	500.	0	0	0	0	0	0	0	0	1,100	
CPP-15	3/1/74	3/4/74	2,000.	1.20E-4	3.00E-6	2.14E-7	5.45E-5	8.39E-6	1.50E-1	2.40E-5	1.67E-2[a]	1.2	
CPP-16	1/1/76	1/7/76	150.	1.10E-3	9.30E-8	1.15E-6	2.94E-4	4.53E-5	6.10E-1	1.30E-4	3.34E-2[a]	7.9	
CPP-20	1/1/58	12/31/77	100.	3.00E-5	2.00E-9	1.14E-8	2.91E-6	4.48E-7	8.00E-3	1.00E-6	0.0E+0[a]	0.23	
CPP-79 (shallow)	7/15/86	7/15/86	2,530.00	0.18	1.40E-4	1.85E-6	4.72E-4	7.27E-5	1.3	2.60E-4	3.52E-8[a]	77	0.
CPP-24	2/1/54	2/1/54	1.00	1.30E-2	6.70E-7	7.12E-12	1.82E-9	2.80E-10	6.00E-6	6.70E-6	1.29E-5[a]	0.023	0.
CPP-25	8/1/60	8/1/60	10.00	2.00E-4	8.10E-8	4.27E-6	1.09E-3	1.67E-4	2.30E-1	4.90E-5	6.95E-5[a]	7	0.
CPP-26	5/1/64	5/1/64	2.00	2.00E-2	1.20E-6	1.08E-5	2.76E-3	4.25E-4	7.6	1.10E-3	6.86E-7[a]	2.6	0.
CPP-30	6/1/76	6/1/76	0.0026	1.50E-6	1.60E-9	9.97E-9	2.54E-6	3.92E-7	7.00E-3	1.10E-6	4.29E-10[a]	0.0015	0.
CPP-32E	12/1/76	12/1/76	0.0008	2.00E-6	4.00E-10	2.85E-9	7.27E-7	1.12E-7	2.00E-3	3.00E-7	2.57E-4[a]	0.0003	0.
CPP-32W	12/1/76	12/1/76	1.00	1.96E-6	5.32E-10	3.45E-9	8.8E-7	1.35E-7	2.32E-3	3.87E-7	6.52E-4[a]	0.00007	0.
CPP-58E 1976	9/1/76	9/15/76	2,500	6.80E-3	1.60E-5	3.70E-10	9.45E-8	1.45E-8	9.40E-5	1.60E-4	1.72E-7[a]	176	0.
CPP-58W	8/1/54	8/1/54	100.00	3.60E-2	3.60E-6	5.13E-11	1.31E-8	2.01E-9	3.60E-5	3.60E-5	2.08E-7[a]	7	0.

a. Early estimate of U-234 source term. The estimate for U-234 developed in Section 5 of the main document was smaller, but the model was not rerun with the latest value because the source term was conservatively larger.

A-9.2.2 Remaining OU 3-13 Sites

Sites CPP-02 and CPP-80 are OU 3-13 liquid release sites. The source estimates for these sites were taken from the OU 3-13 RI/FS and are presented in Table A-9-7. These estimated releases were not revisited during the analysis presented in Section 5 of the main document and may have been overestimated in the OU 3-13 RI/FS. Site CPP-87/89 is a Group 2 site (under Building CPP-649). It was originally identified in the OU 3-14 RI/FS Work Plan (DOE-ID 2004a) as a new site in CPP-58 but has since been more appropriately identified as an OU 3-13 Group 2 site. The source term is developed in Section 5 of the main document (under CPP-58).

Table A-9-7 Remaining OU 3-13 Sources.

Site	First Day	Last Day	Liquid Volume (gal)	H-3 (Ci)	I-129 (Ci)	Np-237 (Ci)	Pu-239 (Ci)	Pu-240 (Ci)	Sr-90 (Ci)	Tc-99 (Ci)	U-234 (Ci)	Nitrate (kg)	Mercury (kg)
CPP-02	1/1/58	12/31/66	4.78E+7	378.1	0.	0.	0.	0.	3.38E+1	0.	0.	0.	0.
CPP-80	1/1/83	12/31/89	1.51E+3	0.	0.	0.	0.	0.	2.75E+2	0.	0.	0.	0.
CPP-87/89 1975	10/1/75	10/14/75	2.50E+3	9.00E-02	9.00E-6	5.84E-10	1.49E-7	2.29E-8	3.40E-4	9.00E-5	6.00E-7[a]	176	0.

a. Early estimate of U-234 source term. The estimate for U-234 developed in Section 5 of the main document was smaller, but the model was not rerun with the latest value because the source term was conservatively larger.

Estimated inventories for the contaminated OU 3-13 soil sites were also taken from the OU 3-13 RI/FS (DOE-ID 1997). These are represented by worst-case scenarios based on measured soil concentrations and site soil volumes. The contaminated soil volume was assumed to be a rectangular box encompassing the surrounding clean soil borings and extending from land surface to the basalt. The contaminant concentration typically assigned to the entire volume corresponded to the maximum value of all samples within each rectangle. As a result, the soil volume was probably overestimated as was the radionuclide inventory. In the model, these sites were incorporated over a 1-day period (March 29, 1996), corresponding to the average date when the samples were collected.

Site CPP-37B is an old gravel pit that received mainly construction debris before it was backfilled. Before 1982, it received waters released from the sludge dewatering pit of the old Sewage Treatment Plant, but the volume is believed to be low (DOE-ID 2004d). In 1991, 26 soil samples were collected from four boreholes approximately every 5 ft to basalt, plus one sample in an interbed at 109 ft deep. Samples were analyzed for inorganics, volatile organic compounds, semivolatile organic compounds, pesticides, herbicides, polychlorinated biphenyls, and radionuclides.

A table of unvalidated data in a draft report (Golder Associates 1992) indicates that 26 samples were analyzed for I-129, 25 of which were nondetect. Only one sample (20 ft deep) had a positive detect for I-129 (1.57 ± 0.82 pCi/g), and it is assumed from reviewing all radionuclide data that the counting error was reported at 2 sigma. From this one sample, the OU 3-13 RI/BRA very conservatively assumed that the entire area of the gravel pit down to bedrock had this concentration of I-129. This calculates to be 3.89×10^{-2} Ci of I-129, which is over 30 times more I-129 than from all of the tank farm sources combined (1.27×10^{-3} Ci). Given that I-129 is highly mobile, was nondetect in all of the 2004 tank farm alluvium samples, and is much more prevalent in tank farm sources (including CPP-31 and CPP-79 [deep]) than CPP-37B sources, the OU 3-13 RI/BRA estimate of the I-129 source term for CPP-37B is too conservative for use in the INTEC model.

Site CPP-37B is a Group 3 (Other Surface Soils) site. The OU 3-13 ROD (DOE-ID 1999) states that modeling and sampling of the site indicated the site is not a significant contributor to groundwater risk or surface exposure risk. No OU 3-13 remediation goals were exceeded (DOE-ID 2004d), including Cs-137, which had a maximum value of 4.2 ± 0.15 pCi/g and Sr-90, which had a maximum concentration of 4.31 ± 0.33 pCi/g. The lack of Sr-90 and Cs-137 contamination also indicates that I-129 should not be a COC for this site.

Site CPP-37B was sampled for I-129 in September of 2005 during ongoing OU 3-13 Group-3 work. There were 11 samples taken and one duplicate. Ten samples were non-detect and 2 were flagged UJ (false positive). The OU 3-13 Group-3 work concluded that the site will not result in unacceptable risk to human health or the environment and that the site will not require further action (personal communication with Dean Shanklin). The Site CPP-37B I-129 was not included as a source term in the revised INTEC model.

At Site CPP-89, the plutonium was reported as total Pu-239/240 as a combined value. This value was used as the Pu-239 source and also for the Pu-240 source, essentially doubling the inventory. Table A-9-8 summarizes the OU 3-13 soil site sources used in the OU 3-14 baseline risk assessment.

Table A-9-8 OU 3-13 contaminated soil sites.

Site	H-3 (Ci)	I-129 (Ci)	Np-237 (Ci)	Pu-239 (Ci)	Pu-240 (Ci)	Sr-90 (Ci)	Tc-99 (Ci)	U-234 (Ci)	Nitrate (kg)	Mercury (kg)
CPP-89	0.	0.	0.	1.18e-1	1.18e-1	9.78e+1	0.	4.95E-2	0.	1.08E+2
CPP-35	0.	0.	0.	9.98e-4	0.	4.46e+0	0.	0.	0.	9.96e+0
CPP-36/91	0.	0.	0.	2.64e-1	0.	5.38e+1	0.	2.29e-3	0.	1.36e+1
CPP-01/04/05	0.	0.	0.	5.88e-2	0.	2.38e+1	0.	0.	0.	0.
CPP-08/09	0.	0.	0.	0.	0.	4.98e-1	0.	0.	0.	0.
CPP-10	0.	0.	0.	0.	0.	2.83e-2	0.	0.	0.	0.
CPP-11	0.	0.	2.57e-4	0.	0.	2.25e-2	0.	2.06e-3	0.	0.
CPP-03	0.	0.	0.	0.	0.	5.59e-1	0.	0.	0.	0.
CPP-17A	0.	0.	0.	0.	0.	7.81e-3	0.	0.	0.	0.
CPP-37A	0.	0.	1.12e-2	0.	0.	8.62e-3	0.	0.	0.	1.08e+1
CPP-37B	0.	0.	6.53e-2	0.	0.	3.58e-1	0.	0.	0.	0.
CPP-14	0.	0.	4.55e-2	0.	0.	7.17e-3	0.	5.02e-2	0.	3.03e+0
CPP-34[a]	0.	0.	1.05e-2	0.	0.	1.88e+2	0.	3.61e-2	0.	0.
CPP-13	0.	0.	0.	0.	0.	5.69e+0	3.68e-3	0.	0.	3.81e-1
CPP-06	0.	0.	0.	0.	0.	3.37e-3	0.	0.	0.	0.
CPP-19	0.	0.	0.	6.13e-1	0.	5.43e+2	0.	0.	0.	6.52e-1
CPP-22	0.	0.	0.	0.	0.	1.38e-1	8.93e-2	0.	0.	0.
CPP-90	0.	0.	0.	0.	0.	6.95e-2	0.	0.	0.	1.07e+1
CPP-93	0.	0.	0.	0.	0.	0.	0.	0.	0.	4.28e+2

a. Site CPP-34 has been remediated but was included in the model.

A-9.2.3 Service Waste

The CPP-3 injection well and former INTEC percolation ponds were used to receive process water and evaporator condensate created during liquid waste calcination. Evaporator condensate is also known as "service waste." The service waste volume and concentrations were taken directly from the OU 3-13 RI/BRA with the exception of the inventories for I-129, Tc-99, and nitrate.

The I-129 discharged into the injection well was taken from the OU 3-13 Group 5 Monitoring Report and Decision Summary (DOE-ID 2004c). The Monitoring Report and Decision Summary reevaluated the inventory of I-129 discharged into the injection well, resulting in a reduction from 1.39 Ci to 0.86 Ci.

Tc-99 concentrations discharged in the service waste were assumed to be equal to the ratio of Tc-99 to I-129 concentrations in the aquifer (DOE-ID 2002) near the CFA in 2001. The current aquifer concentration ratio far south of the INTEC should be representative of the disposal ratio if the two radionuclides are transported identically. Both Tc-99 and I-129 are long-lived and mobile contaminants. The 2001 average aquifer concentration ratio of Tc-99 to I-129 was 13.8 to 1 in wells LF3-10, LF3-08, LF2-09, LF2-08, LF2-11, and CFA-1. This ratio results in a Tc-99 inventory of 12.6 Ci in the service waste. Using this method of estimating, the Tc-99 inventory has limitations because the sorption chemistry and volatility differ between the two radionuclides. However, records of Tc-99 discharges were not kept and significant amounts of Tc-99 were released with the service waste.

The nitrate discharges in the service waste were assumed to be equal to the reported 1981 (Honkus 1982) measured concentrations. That year was chosen because it represents a typical operational year at INTEC and good records of service waste contents were available. The report indicated the average service waste nitrate concentration was 16 µg/mL (as N), which is about 71 mg/L as NO_3-.

The OU 3-13 RI/BRA model applied two average disposal rates to represent the service waste ponds to account for reduced fluxes during the early 1990s. The first rate was taken from disposal records for the period 1984-1990 and the second rate was for the period 1991-1995. The reduction in contaminant flux occurring in the early 1990s occurred as a result of the installation of the Liquid Effluent Treatment and Disposal facility (LET&D), which became operational in January 1993. The LET&D facility removed almost all of the contaminants from the service waste stream. The OU 3-14 model used a single average service waste source term for the period 1984-1993. After 1993, the simulated percolation ponds only received clean water. The service waste source term is summarized in Table A-9-9.

Table A-9-9 Service waste source terms.

COPC	First Day	Last Day	Liquid Volume	H-3 (Ci)	I-129 (Ci)	Np-237 (Ci)	Pu-239 (Ci)	Pu-240 (Ci)	Sr-90 (Ci)	Tc-99 (Ci)	U-234 (Ci)	NO_3- (kg)	Hg (kg)
Injection well (Ci or kg)	12/1/53	3/31/84	Variable	2.01e+4	0.86	1.07	1.35e-2	6.77e-3	2.43e+1	1.19e+1	1.35e-1	2.83e+6	4.00e+2
Percolation pond (Ci or kg)	4/1/84	12/31/93	1.54e+6 (gal/day)	9.99e+2	8.2e-2	0.	1.14e-3	5.71e-4	2.95e-1	1.13e+0	2.15e-2	1.31e+6	0.

A-9.3 Groundwater Simulation Results

Simulation results for the transport of the 10 COPCs are presented in Sections A-9.3.1- A-9.3.9. The transport parameters, federal drinking water standard, slope factor, and background concentration for each COPC is given in Table A-9-10. The constant background concentration was added to the simulation results during the postprocessing. Simulation results are presented first for the vadose zone and then for the aquifer. The overall summary is presented in Section A-9.3.10.

The simulation results are presented in a consistent format for each COPC. The vadose zone simulation results includes the following information: (1) horizontal contour plots of vadose zone concentration at four time periods, (2) vertical contour plots of vadose concentrations at four time periods, (3) time history plot of peak vadose zone concentration, and (4) time history plot of contaminant mass or contaminant activity flux into the aquifer. The aquifer simulation results include the following information: (1) horizontal concentration plots at four time periods and (2) time history plots of peak aquifer concentration. The Sr-90 simulation results are presented in Appendix J along with the geochemical model development. The contaminant concentrations were obtained through simulation in three-dimensions. To present the concentration contours shown in the following sections, these data were reduced by using the maximum concentration at any depth at each horizontal grid block location for the horizontal contour plots. Likewise, the vertical contour plots were created by using the maximum concentration at each vertical grid block location.

This data reduction scheme essentially compresses the contaminant plume in the vertical direction for the horizontal plots and compresses the contaminant plume in the east/west direction for the vertical plots. The vadose zone contour intervals are presented for each order of magnitude above and below the Snake River Plain Aquifer MCL, with the range spanning 10^{-1} * Snake River Plain Aquifer MCL to 10^{1} * Snake River Plain Aquifer MCL. The concentration isopleths below, equal to, and above the Snake River Plain Aquifer MCL are denoted by thin black lines, a thick red line, and thin red lines, respectively. The background concentrations for Orr et al. (1991) for each COPC were added to the vadose zone and aquifer simulations results. The aquifer contour intervals include a 10^{-2} * Snake River Plain Aquifer MCL isopleth, which is denoted by a thin dashed black line.

Table A-9-10 Contaminants of potential concern summary.

COPC	Half-Life (years)	Vadose Zone Alluvium K_d (mL/g)	Vadose Zone Interbed K_d (mL/g)	Vadose Zone Basalt K_d (mL/g)	Aquifer Interbed K_d (mL/g)	Aquifer Basalt K_d (mL/g)	SRPA MCL (pCi/L or mg/L)	Slope Factor (1/pCi)	Background Concentration (pCi/L or mg/L)
H-3	1.23e+1	0.	0.	0.	0.	0.	20,000.	5.07e-14	100.
I-129	1.57e+7	1.5	0.7	0.	0.7	0.	1.	1.48e-10	0.05
Np-237	2.14e+6	2.	2.	0.	2.	0.	15.	6.18e-11	0.
Pu-239	2.41e+4	1,000.	1,000.	0.	1,000.	0.	15.	1.35e-10	0.
Pu-240	6.57e+3	1,000.	1,000.	0.	1,000.	0.	15.	1.35e-10	0.
Sr-90	2.86e+1	Variable[a]	50.[b]	0.	1.34	0.038	8.	5.59e-11	0.1
Tc-99	2.13e+5	0.	0.	0.	0.	0.	900.	2.75e-12	0.
U-234	2.44e+5	1.6	1.6	0.	1.6	0.	0.03 (mg/L)	7.07e-11	0.000002 (mg/L)[c]
Mercury	none	118	156	0.	156	0.	0.002	3.0e-4	0.0001
Nitrate	none	0.1	0.1	0.	0.1	0.	10.	None	1.5
a. The geochemical model presented in Appendix J was used to estimate initial Sr-90 transport and residual K_d.									
b. The interbed Sr-90 K_d value prensented in Appendix D was revised in Appendix J.									
c. Total uranium background concentrations were taken from Roback et al., (2001).									

A-9.3.1 H-3

The sources of tritium in the vadose zone, listed in order of decreasing magnitude, are (1) service waste ponds at 999 Ci, (2) CPP-3 injection well failure at 708 Ci, (3) CPP-02 site at 378 Ci, and (4) the tank farm sources at 9.7 Ci. The tritium released directly into the aquifer through the injection well was 1.94e+4 Ci, which is orders of magnitude greater than that released in the tank farm.

A-9.3.1.1 Vadose Zone H-3 Simulation Results

Figures A-9-2 and A-9-3 illustrate the horizontal and vertical distribution of tritium in the vadose zone at four time periods: 1979, 2005, 2049, and 2095. The concentration isopleths are presented in Figures A-9-2 and A-9-3. Figure A-9-4 presents the peak vadose zone concentrations through time (excluding the tank farm submodel area), and Figure A-9-5 illustrates the tritium activity flux into the aquifer.

Tritium concentrations drop quickly in the vadose zone because it is nonsorbing and because it has a short (12.3-year) half-life. The vadose zone concentrations are highest in central and southern INTEC as a result of the CPP-3 injection well failure and the service waste ponds. The highest tritium concentration occurred in 1965 as a result of the CPP-02 site, which is the former french drain located in southern INTEC. The injection well failure results in a large initial arrival in the aquifer during the early 1970s, and the percolation pond operation results in a later and smaller arrival during the 1980s to early 1990s. The simulated tritium concentrations in the northern shallow perched water were similar in magnitude to the observed concentrations. However, simulated tritium concentration in the northern deep perched water were lower than observed in well MW-18 and USGS-50.

A-9.3.1.2 Aquifer H-3 Simulation Results

Figure A-9-6 illustrates the horizontal distribution of aquifer tritium at four time periods: 1979, 2005, 2049, and 2095. Figure A-9-7 presents the peak aquifer concentrations through time.

The highest aquifer concentrations were the result of the CPP-3 injection well operation. The peak aquifer tritium concentration was 4.02e+6 pCi/L in 1965. The simulated tritium concentrations exceeded the Snake River Plain Aquifer MCL from 1954 to 2001. The current location of the highest tritium concentrations are near the CFA. The tritium contamination currently beneath INTEC is most likely from tritium discharged to the percolation ponds and other vadose sources. These sources are now entering the aquifer.

Figure A-9-2. H-3 horizontal vadose zone concentrations (pCi/L) (SRPA MCL = thick red line, 10*SRPA MCL = thin red line, SRPA MCL/10 = thin black line).

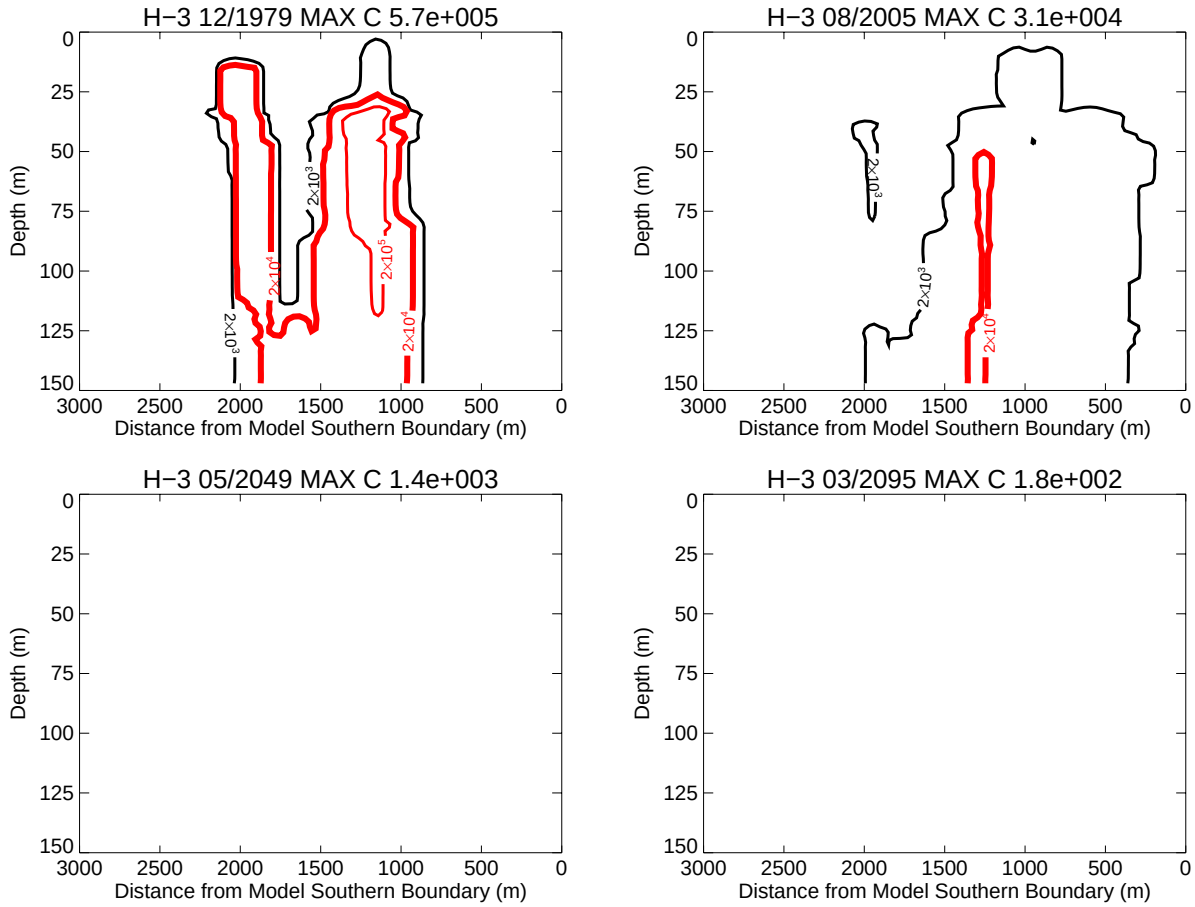

Figure A-9-3. H-3 vertical vadose zone concentrations (pCi/L) (SRPA MCL = thick red line, 10*SRPA MCL = thin red line, SRPA MCL/10 = thin black line).

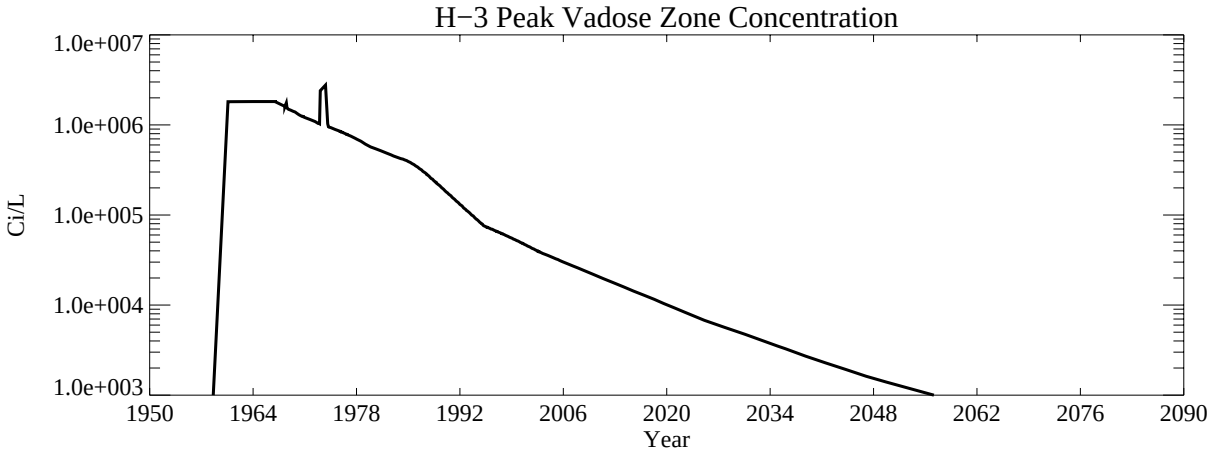

Figure A-9-4. H-3 peak vadose zone concentrations excluding tank farm submodel area (pCi/L) (SRPA MCL = blue, model predicted = black line).

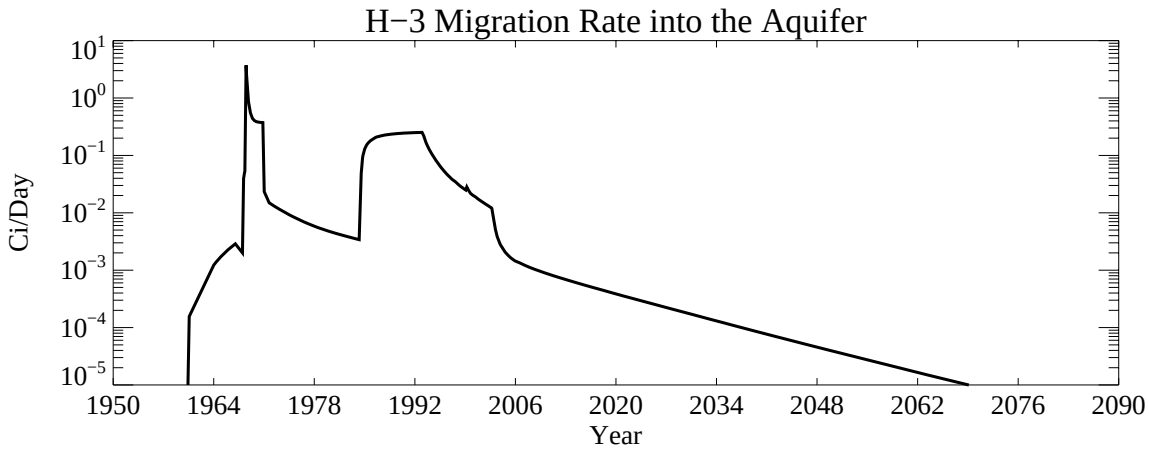

Figure A-9-5. H-3 peak activity flux into the aquifer (Ci/day).

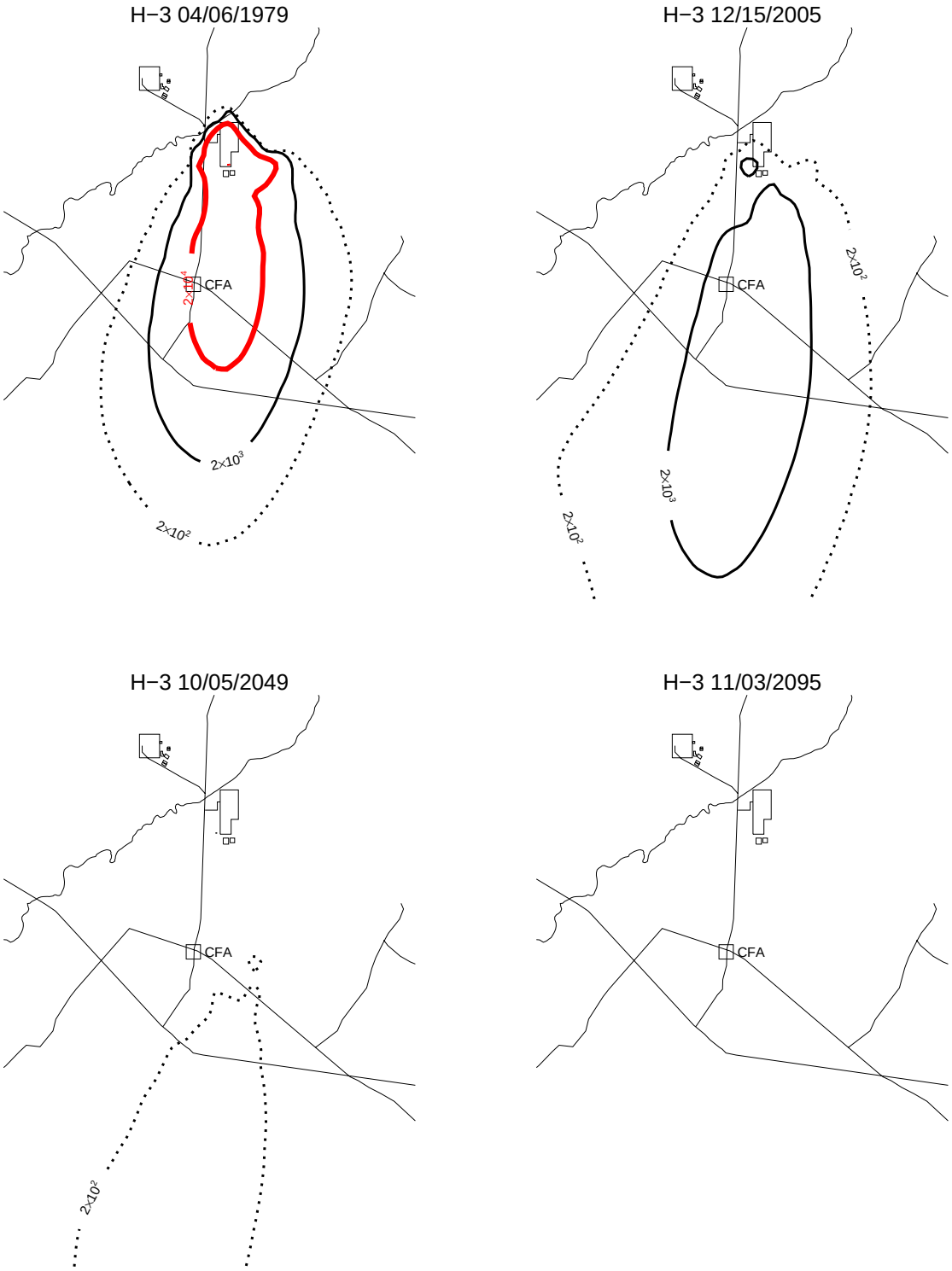

Figure A-9-6. H-3 horizontal aquifer concentrations (pCi/L) (SRPA MCL = thick red line, 10*SRPA MCL = thin red line, SRPA MCL/10 = thin black line, SRPA MCL/100 = thin black dashed line).

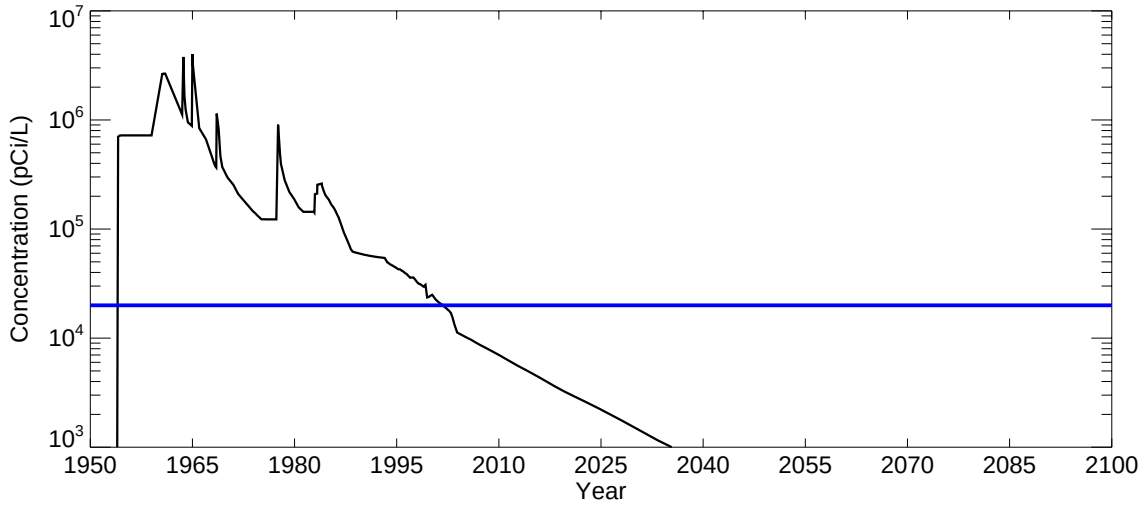

Figure A-9-7. H-3 peak aquifer concentrations (pCi/L) (SRPA MCL = blue line, model predicted = black line).

A-9.3.2 I-129

The sources of I-129 in the vadose zone, listed in order of decreasing magnitude, are (1) CPP-3 injection well failure at 0.08 Ci, (2) service waste ponds at 0.082 Ci, (3) OU 3-13 soil sources at 0.039 Ci, and (4) the tank farm sources at 0.00126 Ci. The I-129 released directly to the aquifer from the injection well was 0.78 Ci.

A-9.3.2.1 Vadose Zone I-129 Simulation Results

Figures A-9-8 and A-9-9 illustrate the horizontal and vertical location of the vadose zone I-129 at four time periods: 1979, 2005, 2049, and 2095. Figure A-9-10 presents the peak vadose zone concentrations through time (excluding the tank farm submodel area), and Figure A-9-11 illustrates the I-129 peak activity flux into the aquifer.

Like tritium, the majority of the I-129 originates from the service waste discharged into the CPP-3 injection well and the service waste ponds. The simulated I-129 is widespread in the central INTEC deep vadose zone water during the injection well failure period and widespread in the southern vadose zone during the percolation pond operation. The peak simulated vadose zone concentration (excluding the tank farm submodel area) was 30 pCi/L in 1971.

A-9.3.2.2 Aquifer I-129 Simulation Results

Figure A-9-12 illustrates the horizontal distribution of I-129 in the aquifer in 1979, 2005, 2049, and 2095. Figure A-9-13 presents the peak aquifer concentrations through time. Like tritium, the highest simulated aquifer I-129 concentrations were the result of the CPP-3 injection well operation. The peak aquifer I-129 concentration was predicted to be 22.6 pCi/L and occurred in 1970 from the service waste disposed of in the CPP-3 injection well.

The I-129 concentrations were predicted to exceed the Snake River Plain Aquifer MCL from 1954 to 2080. The peak simulated concentration in the year 2095 was 0.9 pCi/L. The current simulated location of the highest I-129 concentrations are near the CFA, and the source is from I-129 discharged into the CPP-3 injection well and former percolation ponds. The general trend of the model is to overpredict aquifer I-129 concentrations. The highest three measured concentrations reported in the 2004 Group 5 monitoring report

(DOE-ID 2006) were 0.772, 0.615, and 0.608 pCi/L in wells USGS-47, USGS-57, and LF3-08, respectively. The model predicts concentrations near LF3-9 to be 0.9 pCi/L, but also predicts concentrations at LF2-11 (located approximately 1,200 m northeast of LF3-9) to be near 4 pCi/L in 2005. The most recent measured concentration was in well LF2-11 and was 0.98 pCi/L in 2001. The model could be overpredicting current maximum concentrations by approximately factor of four.

Figure A-9-8. I-129 horizontal vadose zone concentrations (pCi/L) (SRPA MCL = thick red line, 10*SRPA MCL = thin red line, SRPA MCL/10 = thin black line).

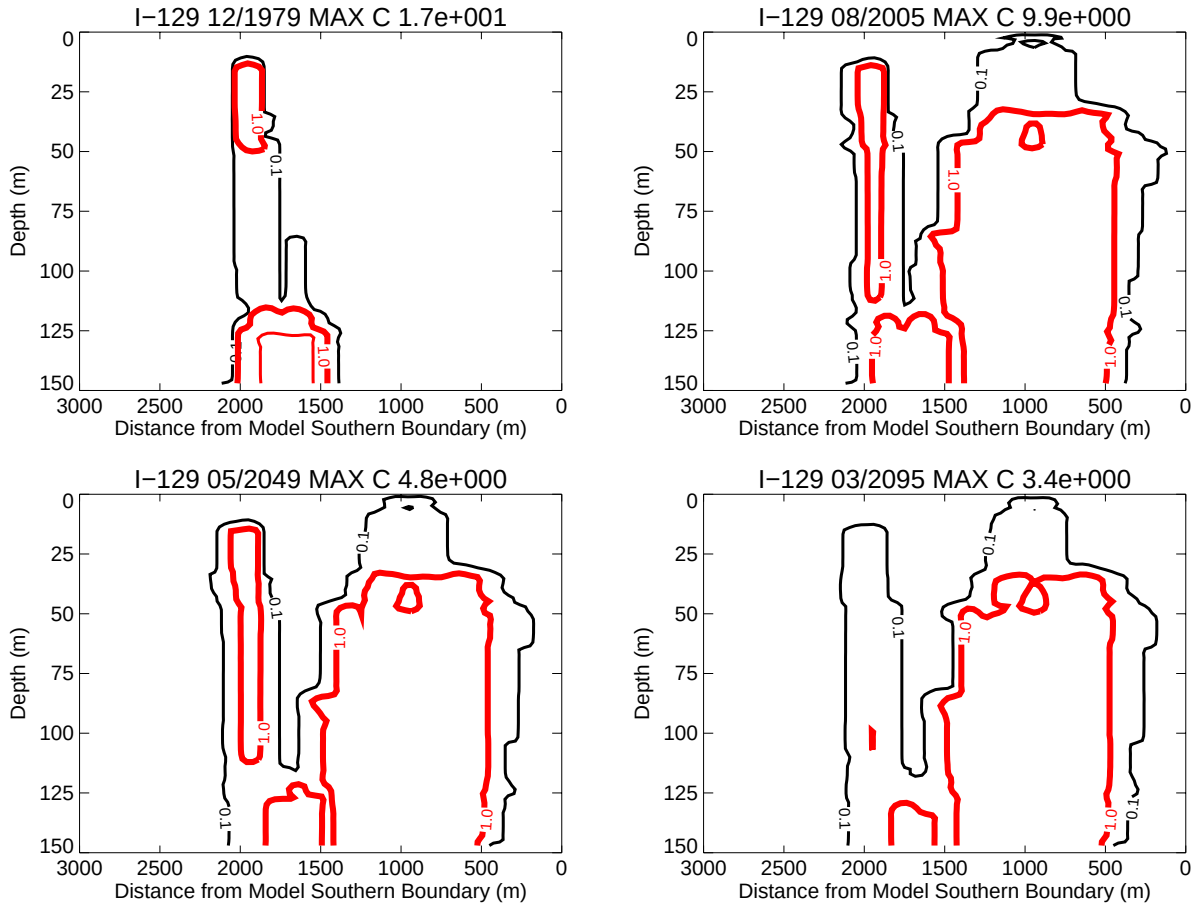

Figure A-9-9. I-129 vertical vadose zone concentrations (pCi/L) (SRPA MCL = thick red line, 10*SRPA MCL = thin red line, SRPA MCL/10 = thin black line).

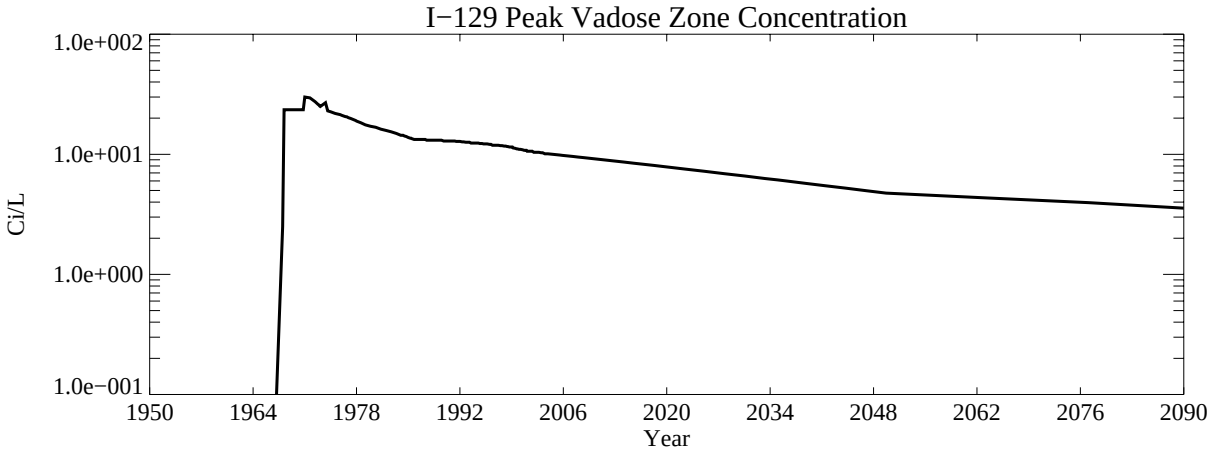

Figure A-9-10. I-129 peak vadose zone concentrations excluding tank farm submodel area (pCi/L).

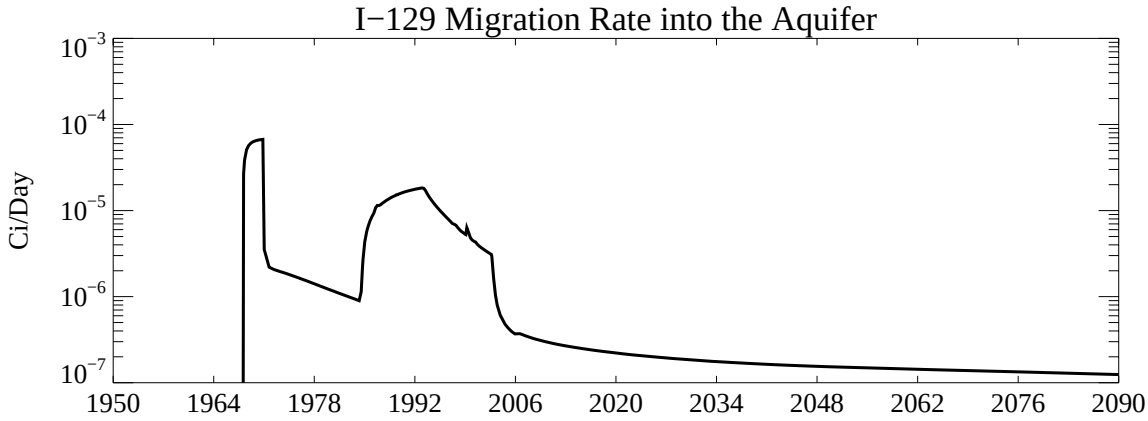

Figure A-9-11. I-129 peak activity flux into the aquifer (Ci/day).

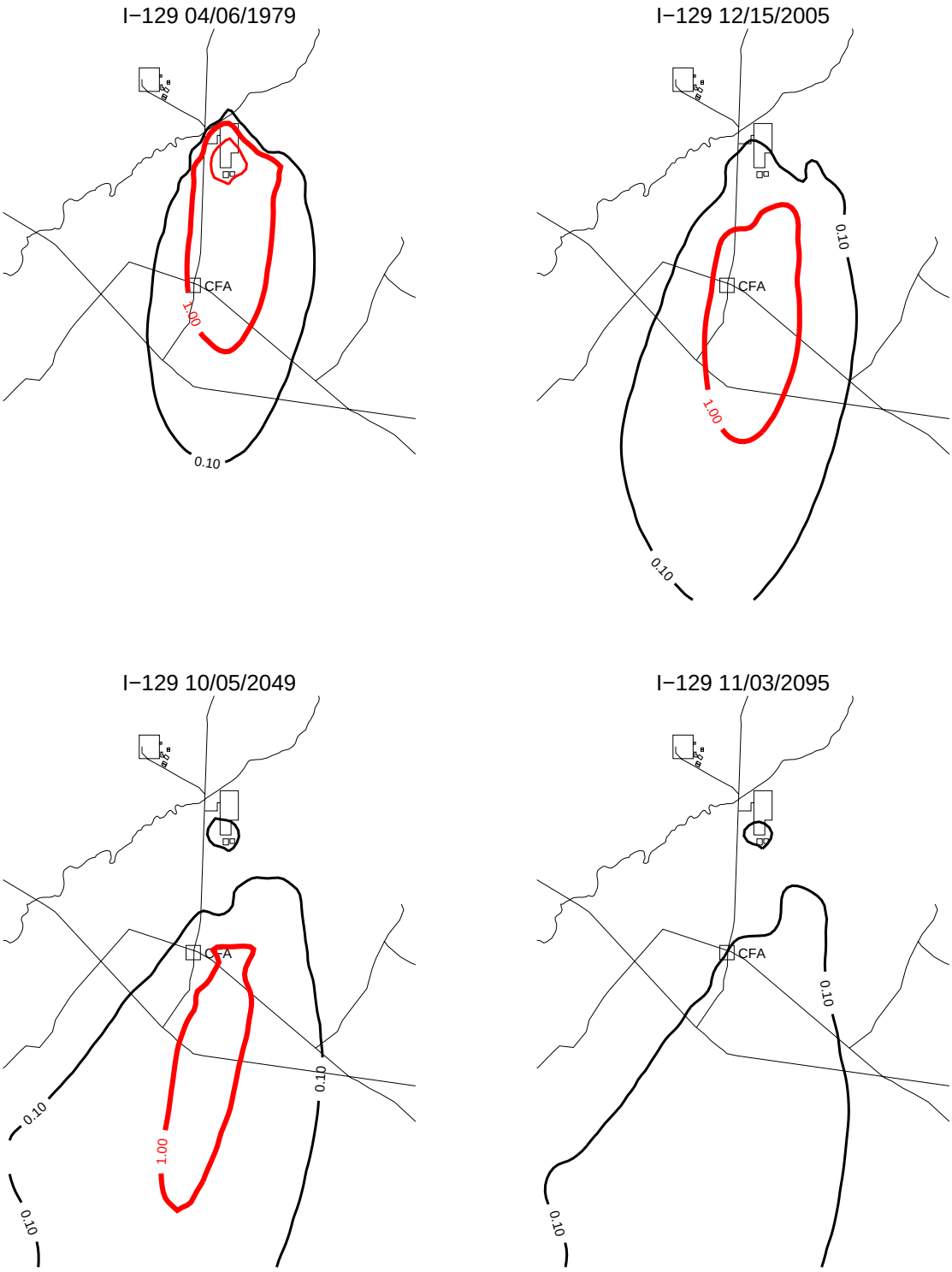

Figure A-9-12. I-129 horizontal aquifer concentrations (pCi/L) (SRPA MCL = thick red line, 10*SRPA MCL = thin red line, SRPA MCL/10 = thin black line, SRPA MCL/100 = thin black dashed line).